

**INCORPORATION OF MICROBIAL BIOMASS
INTO A MODEL OF EARLY DIAGENESIS**

By

Patrick Schultz

A THESIS

Submitted in partial fulfillment of the requirements for the degree of
MASTER OF SCIENCE IN ENVIRONMENTAL ENGINEERING

MICHIGAN TECHNOLOGICAL UNIVERSITY

2002

© Patrick Schultz 2002

This thesis

**“INCORPORATION OF MICROBIAL BIOMASS
INTO A MODEL OF EARLY DIAGENESIS”**

is hereby approved in partial fulfillment of the requirements for the degree
of MASTER OF SCIENCE IN ENVIRONMENTAL ENGINEERING.

DEPARTMENT: Civil and Environmental Engineering

Thesis Advisor: _____

Typewritten Name: _____

Department Chair: _____

Typewritten Name: _____

Date: _____

For my parents Christl and Horst

Abstract

Sediments in many lakes and reservoirs are characterized by spatial heterogeneity of their properties and highly variable inputs of organic matter on time scales ranging from days to decades. Predictions of sediment nutrient release rates as needed in many water quality models have to account for this variability in space and time. The first section of this thesis (Introduction) gives background information on the Croton Watershed, part of New York City's drinking water system. The Croton reservoir system is used to illustrate the importance of sediment processes for surface water quality modeling and to determine objectives for the development of a refined model of early diagenesis.

The second section (Article), a manuscript to be submitted to the Journal of Environmental Quality, focuses on the effects of microbial biomass on sediment nutrient release and the incorporation of microbial biomass into a model of organic matter decomposition in sediments. For this study, a new model of early diagenesis (BIOSED), which explicitly includes microbial biomass as a state variable, was developed. Model predictions of sediment C and N release are compared to the commonly used, first-order, multi-G model, and the effects of changes in microbial biomass on nutrient mineralization are examined. The new model leads to substantially different predictions of N release in sediments with low organic C content. The model predicts that over short time periods microbial biomass dampens oscillations in N release rates and over longer periods of eutrophication, immobilization of N into microbial biomass reduces N mineralization.

Model simulations also suggest that the microbial biomass pool size and the rate of organic matter decomposition are closely linked to substrate quality. Anaerobic incubation experiments were conducted to better understand the role of different substrates in nutrient recycling. Amendment of sediment with labile substrate (i.e., fresh algae, amino acids) is shown to be a useful method to assess organic matter quality in sediments. The fraction of organic C associated with labile substrate varied greatly among surface grab samples of lake sediments (2-10%). In contrast with other studies, organic N seemed to be readily accessible for microbial breakdown and primarily bound to labile material in all sediment samples.

The third section (Appendices) shows additional work that was conducted as part of this research project. Detailed methods and results from the Croton Watershed study are presented in Appendix 1, the model framework is discussed in more detail in Appendix 2, and Appendix 4 contains additional results from the incubation experiments and a brief discussion of experimental concerns. Experimental protocols (App. 3) and Visual Basic code for the two-box BIOSSED model (App. 5) are also included.

Acknowledgements

My studies at Michigan Tech have been an invaluable learning experience, and many people have contributed to the completion of my research project and my Master's degree. First of all, I want to thank my advisor, Dr. Noel Urban. Our weekly discussions and his constant feedback throughout all phases of the project have been crucial in shaping this thesis. Dr. Urban's knowledge of sediment processes and his passion for biogeochemical cycles were essential for my understanding of the subject and my motivation. I would also like to thank the other committee members, Dr. Auer, Dr. Jurgensen, and Dr. Mayer, for their time and efforts in reviewing this manuscript.

The experimental part of my project would not have been possible without the help and advice from numerous people in Biology, Forestry, and Civil and Environmental Engineering. Thank you very much! Special thanks go to Dave Perram for sharing his expertise and lab equipment and, of course, to Cory Larsen for endless hours of glassware washing.

Studying abroad is a big adventure and it was made possible for me through the efforts and support of several people and organizations in both Germany and the United States. Prof. Kobus, Prof. Rott, and Andreas Sihler at the University of Stuttgart provided advice and help in organizing the combination of my Master's studies with the "Diplom-Ingenieur" degree. In addition, I would like to acknowledge the German National Merit Foundation, the German-American Fulbright Commission, and the Michigan Tech Graduate School for their financial support. I am especially thankful to Dr. Peter Schaefer for generously sponsoring my scholarship.

Successful studies also depend on the quality of life and the value of the breaks from work. Finding distraction, celebrating the small victories of everyday-life, and having fun even without obvious reasons to celebrate was always easy with the help of the many new friends I made at Tech. Keep in touch, I will miss your company!

Last but not least, I want to thank the people who are closest to my heart even if they are far away. A big thanks goes to my parents and my sister for their love and support. You taught me curiosity and persistence, the basis of any research! Finally, I want to thank Pooja Sharma. Together with you, Houghton was more than just a place to live, it became a home.

Table of contents

Abstract	iv
Acknowledgements	vi
Table of contents	vii
List of Figures	ix
List of Tables	xi
1. Introduction	1
Surface Water Quality Modeling	2
2. Article	10
Abstract	11
Introduction	12
Model Framework	15
Box-Models	15
Decomposition kinetics	17
Methods	20
Sediment collection	20
Anaerobic incubations	21
Analyses	22
Model simulations	23
Results	25
Sediment C and N contents	25
Incubation experiments	26
Steady-state	29
Time-dependent simulations	32
Two-Box model	33
Discussion	35
Substrate Quality	35
Biomass pool size	38
Water quality modeling	41
3. Appendices	44
Appendix 1: Croton Watershed sediments	45
A) Stratigraphy of New Croton Reservoir Sediments	45
B) Sediment-water exchange rates	53
Appendix 2: Model Framework	59
Box-Models	59
Decomposition kinetics	61
Reference Scenario	65
Mathematical representation	69

Appendix 3: Experimental Protocols	76
Sediment amendments, Sample preparation	76
Take and process incubation samples	77
Ammonia measurements	79
Titration (alkalinity, ΣCO_2)	80
Protocol: Algae culture	81
Appendix 4: Additional experimental results	82
Experimental concerns	82
DIC and DIN concentrations	83
Substrate quality and C and N release rates	85
Appendix 5: Visual Basic Code	93
Two-Box BIOSED model	93
4. References	100

List of Figures

Introduction

Figure 1-1 – Location of the Croton Watershed	3
Figure 1-2 – New Croton Reservoir: Comparison of porosity at stations 1, 4, 5	6
Figure 1-3 – New Croton Reservoir: Comparison of loss on ignition at stations 1, 4, 5	7
Figure 1-4 – New Croton Reservoir: Sediment profiles of C:N ratios at stations 1, 4, and 5	7

Article

Figure 2-1 – Two-box model framework	16
Figure 2-2 – All sediments: Percentage of sediment C released as DIC per day	28
Figure 2-3 – All sediments: Percentage of sediment N released as DIN per day	28
Figure 2-4 – Model: Effect of varying C uptake efficiency on biomass pool size	30
Figure 2-5 – Model: Effect of varying C uptake efficiency on N release rate	30
Figure 2-6 – Model differences in N release rates as a function of organic matter input	31
Figure 2-7 – Model: Effect of sediment C:N ratio on release C:N ratio	31
Figure 2-8 – Model: Long-term eutrophication: Differences in N release	32
Figure 2-9 – Model: Short-term sedimentation event (algae bloom): N release rate	33
Figure 2-10 – Two-Box BIOSSED model: POC fluxes between water and sediment, between boxes, and burial flux.	34
Figure 2-11 – Unamended sediments: N release rates vs. sediment N content	36
Figure 2-12 – Estimation of the labile C pool using sediment amendment experiments	38
Figure 2-13 – BIOSSED: Change in microbial biomass with varying organic matter input	40

Appendices

Figure 3-1 – New Croton reservoir: C content vs. Loss-on-Ignition (LOI)	46
Figure 3-2 – New Croton Reservoir: Comparison of porosity at stations 1, 4, 5	48
Figure 3-3 – New Croton Reservoir: Comparison of sediment bulk density at stations 1, 4, 5	48
Figure 3-4 – New Croton Reservoir: Comparison of loss on ignition at stations 1, 4, 5	49
Figure 3-5 Profile of sediment C, N, and P content for New Croton Reservoir Station 1.	49
Figure 3-6 – New Croton Reservoir: Profiles of sediment C, N and P for Station 4	50
Figure 3-7 – New Croton Reservoir: Profiles of sediment C, N and P for Station 5	50
Figure 3-8 – New Croton Reservoir: Sediment profiles of C:N ratios at stations 1, 4, and 5	51
Figure 3-9 – New Croton Reservoir: Sediment profiles of total iron at stations 1, 4, 5	52
Figure 3-10 – New Croton Reservoir: Sediment profiles of Mn content at stations 1, 4 and 5	52
Figure 3-11 – New Croton Reservoir Station 1: Example of SOD measurements	56
Figure 3-12 – New Croton Reservoir Station 5: Release of NH ₃ -N from sediments	56
Figure 3-13 – New Croton Reservoir Station 1: P release from sediments under both oxic and anoxic conditions	57
Figure 3-14 – New Croton Reservoir Station 5: Release of Fe ²⁺ and Mn ²⁺ under anoxic conditions	57
Figure 3-15 – New Croton Reservoir Station 5: Exchange of color and DOC above sediments	58

<i>Figure 3-16 – Chassell Bay: DIC release</i>	88
<i>Figure 3-17 – Chassell Bay: DIN release</i>	88
<i>Figure 3-18 – Lily Pond: DIC release</i>	88
<i>Figure 3-19 – Lily Pond: DIN release</i>	88
<i>Figure 3-20 – Sturgeon Sloughs: DIC release</i>	88
<i>Figure 3-21 – Sturgeon Sloughs: DIN release</i>	88
<i>Figure 3-22 – Dollar Bay (DBC): DIC release</i>	89
<i>Figure 3-23 – Dollar Bay (DBC): DIN release</i>	89
<i>Figure 3-24 – Dollar Bay (DBLG): DIC release</i>	89
<i>Figure 3-25 – Dollar Bay (DBLG): DIN release</i>	89
<i>Figure 3-26 – Dollar Bay (DBSG): DIC release</i>	89
<i>Figure 3-27 – Dollar Bay (DBSG): DIN release</i>	89
<i>Figure 3-28 – Dollar Bay (DBA): DIC release</i>	90
<i>Figure 3-29 – Dollar Bay (DBA): N release</i>	90
<i>Figure 3-30 – Relationship between dissolved and adsorbed ammonium</i>	90
<i>Figure 3-31 – Unamended sediments: C release rates</i>	91
<i>Figure 3-32 – Amended sediments: C release rates</i>	91
<i>Figure 3-33 – Unamended sediments: N release rates</i>	91
<i>Figure 3-34 – Amended sediments: N release rates</i>	91
<i>Figure 3-35 – Amended sediments: Increase in DIC flux vs. increase in sediment C content</i>	92
<i>Figure 3-36 – Amended sediments: Increase in N flux vs. increase in sediment N content</i>	92

List of Tables

Article

<i>Table 2-1 – Properties of unamended and amended sediments</i>	26
<i>Table 2-2 – Carbon release rates (per sediment dry weight)</i>	27
<i>Table 2-3 – Nitrogen release rates (per sediment dry weight)</i>	27

Appendices

<i>Table 3-1 – Differential equations: two-box multi-G model</i>	69
<i>Table 3-2 – Differential Equations: two-box BIOSED model</i>	70
<i>Table 3-3 – Analytical solution: two-box multi-G model</i>	71
<i>Table 3-4 – Analytical solution: two-box BIOSED model</i>	72
<i>Table 3-5 – Common model parameters (multi-G, BIOSED)</i>	73
<i>Table 3-6 – Specific model parameters (BIOSED model)</i>	74
<i>Table 3-7 – Reference scenario</i>	74
<i>Table 3-8 - One-box steady-state pools and fluxes (reference scenario)</i>	75

1. Introduction

Surface Water Quality Modeling

The Croton watershed is an integral part of New York City's drinking water system. It is located east of the Hudson River and covers approximately 375 square miles of mostly forested land (Figure 1-1). Normally, the twelve reservoirs in the Croton watershed provide drinking water for 10 to 12 % of New York City's population; under drought conditions the percentage may double. In recent years, increased external nutrient loadings have led to the eutrophication of the reservoirs. The resultant deterioration of the water quality in the system is an ecological and economical concern. Due to algal blooms, the New Croton Reservoir had to remain offline for approximately 16% of the time over a six year period (1990-1995). In times of less severe algal blooms that do not warrant a complete shutdown of the system, increased algal levels can impair drinking water disinfection. Prolonged phases of anoxia in the bottom waters of the reservoirs as a result of eutrophication cause additional problems for the drinking water quality. Poor water color, taste and odor are commonly related to high bacterial concentrations and to the release of iron, manganese, and hydrogen sulfide under anaerobic conditions (NYS, 2000).

To prevent further impairment of the drinking water supply from the Croton watershed, the construction of a filtering plant has been proposed for 2007. However, associated costs and the perception that filtration as an end-of-the-pipe technology would contradict efforts to restore the water quality through watershed management have caused much controversy. The development of a comprehensive water quality model for the entire Croton reservoir system by the Upstate Freshwater Institute will yield a better understanding of system-wide biogeochemical processes. This insight will be used to

assess scientifically the need for a filtering plant and to develop an improved management practice. The study presented here contributes to the development of a refined model of early diagenesis that can be incorporated into the overall water quality model.

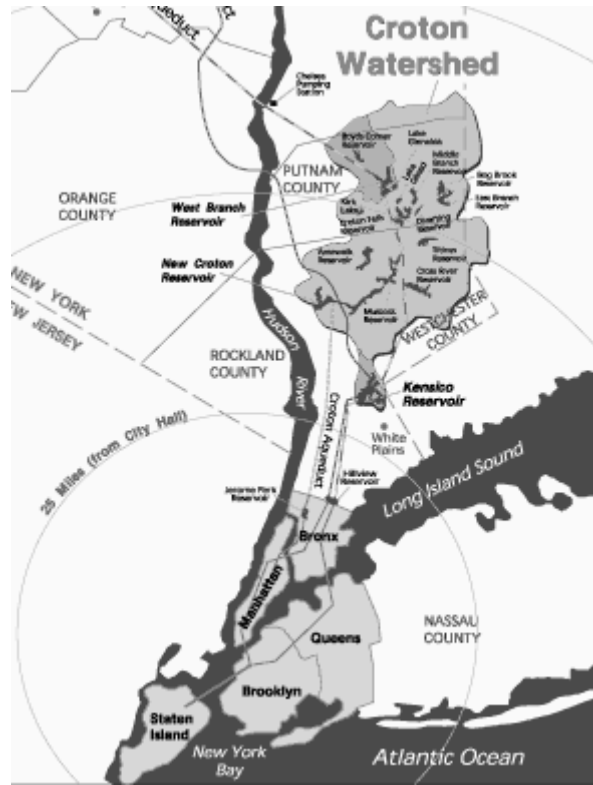


Figure 1-1 – Location of the Croton Watershed (NYC-DEP, 2000)

Simulation models such as that developed here are valuable tools to integrate quantitatively the diverse physical, chemical, and biological processes that define complex environmental systems. Thus, they are not only a cost-effective way of solving particular contamination problems, but also a means for understanding how the environment works as a unit (CHAPRA, 1997). In this study modeling is used as a tool to better understand the kinetics of organic matter decomposition and its effects on sediment nutrient release. Results are not specific to one location but generally applicable to a wide

range of sediments. An extensive data set from the New Croton Reservoir containing sediment properties and nutrient release rates is used to exemplify conditions under which a refined model of early diagenesis may be needed. Detailed methods and results from the New Croton study are shown in Appendix 1; the most pertinent implications of these measurements are discussed below.

Diagenetic processes within lake and reservoir sediments are closely linked to the overlying water column. On the one hand, sediment stratigraphy provides valuable information on the current state of the lake as well as historical changes within the lake and the watershed. Catchment size, lake morphometry, trophic status, and hydraulic regime of the lake are reflected in sediment properties (GORHAM et al., 1983; GORHAM et al., 1974; TARTARI and BIASCI, 1997). On the other hand, mineralization of nutrients from deposited organic matter in the sediments and subsequent release of inorganic nutrients to the water column is an important feedback mechanism for the trophic status of the lake or reservoir. Internal phosphorus loading resulting from sediment phosphorus release can account for up to 80% of total P inputs to some lakes (LARSEN et al., 1981). If external P loadings are reduced in an effort to restore surface water quality, lake recovery can be significantly retarded by persistently high sediment release rates (LARSEN et al., 1981; ROSSI and PREMAZZI, 1991; WELCH et al., 1986). Moreover, sediment oxygen demand as a result of oxygen-consuming processes in the sediments is usually the primary cause for summertime anoxia in the hypolimnion of some lakes and reservoirs (DI TORO, 2001; THOMANN and MUELLER, 1987). Clearly, water quality models must include these interactions between sediments and the water column.

However, to date no models are available that predict sediment nutrient release rates *a priori*. Rates of sediment-water exchange are commonly measured directly (e.g., ERICKSON and AUER, 1998; URBAN et al., 1997), and values feed into the models of water quality as constant parameters. Estimation of release rates based on models applied to profiles of measured sediment properties (e.g., PENN et al., 1995; WANG and VAN CAPPELLEN, 1996) is another commonly used approach. The applicability of both methods for water quality models and their use in reservoir management hinge on two factors. Firstly, both methods depend on point measurements. Site-specific rates of sediment-water exchange must be spatially extrapolated to the entire lake or reservoir area. Although models have been developed to extrapolate point measurements of sediment accumulation rates to entire basins (e.g., ENGSTROM et al., 1994; URBAN et al., 2001), these models have not been evaluated for prediction of sediment fluxes (URBAN et al., 1997). Secondly, the incorporation of constant rates of sediment-water exchange into water quality models implicitly assumes steady-state. Seasonal variations and long-term variability (e.g., due to cultural eutrophication) in sediment fluxes are not captured by one-time measurements. Refinements in early diagenesis modeling as a component of a comprehensive water quality model should therefore include an accurate spatial representation of sediment properties and fluxes as well as dynamic behavior on different time scales (days – years).

Sediment stratigraphy data from the New Croton reservoir provides excellent examples for both spatial and temporal variability in sediment processes. Measurements of porosity, bulk density, and loss-on-ignition (i.e., volatile solids) for seven sediment cores from three stations within the New Croton reservoir show markedly different

patterns for pelagic sediments (Station 1 and 5) and littoral sediments (Station 4). Pelagic stations are characterized by high porosity (> 75%) and high concentrations of volatile solids (15-25%), whereas station 4 has coarser sediments with much lower porosity (<50%) and a lower loss-on-ignition (<10%) (Figure 1-2, Figure 1-3). Elemental analyses (total C, total N, total P) of one sediment core from each station confirm these findings. The profiles of C:N ratios at stations 1 and 5 are nearly constant in the typical range of poorly decomposed autochthonous organic matter (8-10, URBAN et al., 2002) and indicate that the input of organic matter at these stations is dominated by settling algal material with very little input of terrestrial organic matter. In contrast, the organic matter at station 4 has a significantly higher C:N ratio suggesting high inputs of more refractory material derived from macrophytes and terrestrial plants (Figure 1-4). Consequently, rates of sediment-water exchange at littoral station 4 are likely to be considerably different than at the deep-water stations 1 and 5. Moreover, depth profiles at stations 1 and 5 reveal an apparent change in historical conditions.

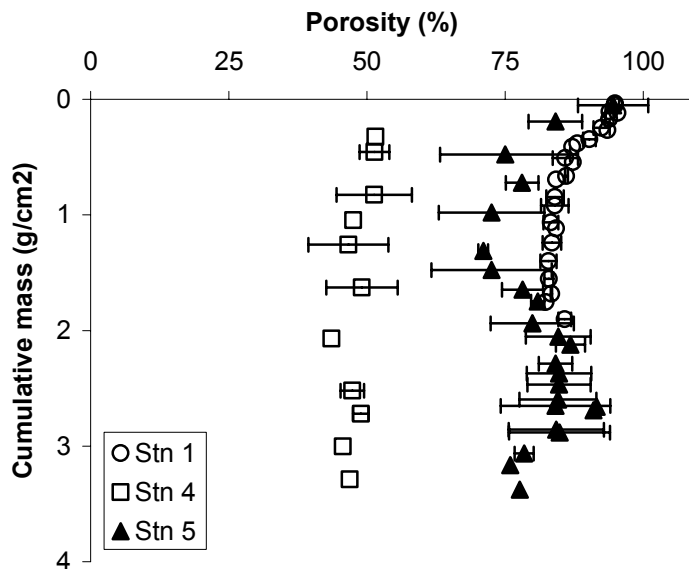


Figure 1-2 – New Croton Reservoir: Comparison of porosity at stations 1, 4, 5 (water content; error bars = ± 1 standard deviation)

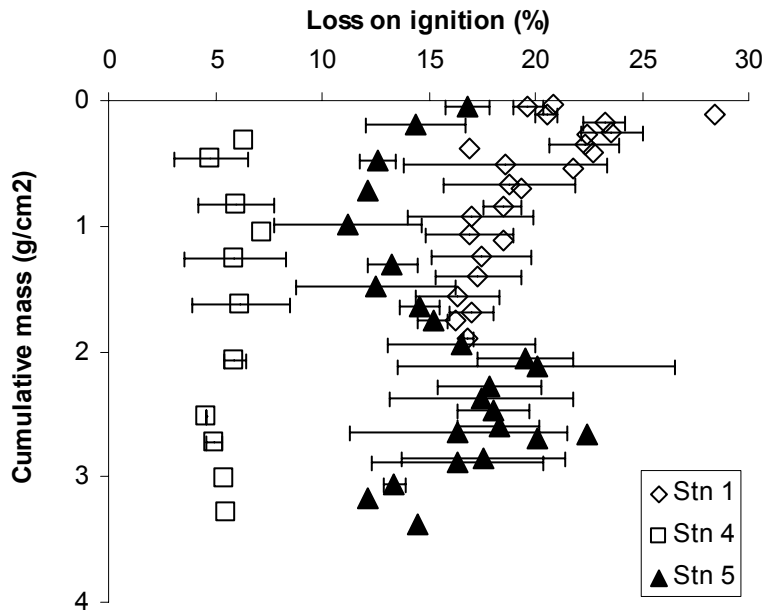


Figure 1-3 – New Croton Reservoir: Comparison of loss on ignition at stations 1, 4, 5 (error bars = ± 1 standard deviation)

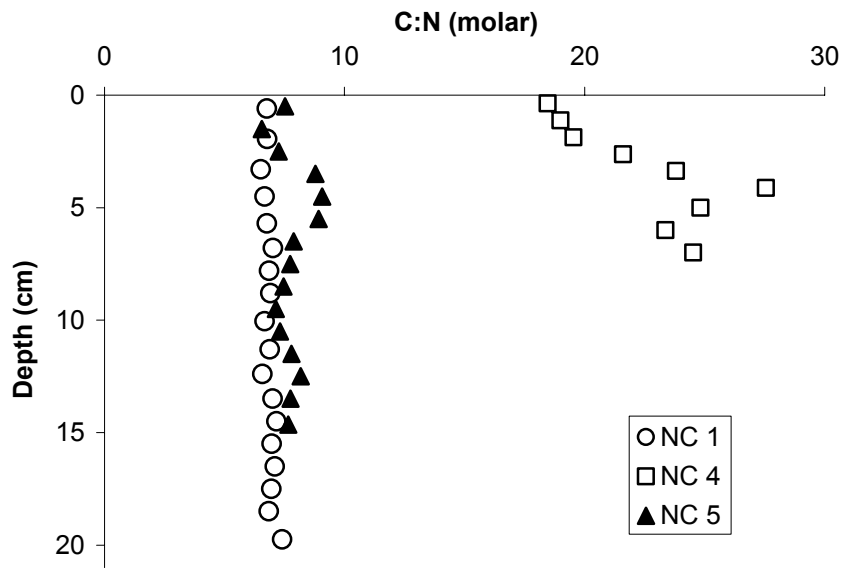


Figure 1-4 – New Croton Reservoir: Sediment profiles of C:N ratios at stations 1, 4, and 5

The differences in sediment composition at the three stations are reflected in different exchange rates as well. Station 4 is characterized by high sediment oxygen demand (SOD), low oxic rates of P and N release, and dramatic differences in release rates under oxic and anoxic conditions. Although station 4 has a low organic matter content per unit mass of sediments, other researchers have found that the organic matter content per unit volume in coarse-grained sediments is similar to that of fine-grained sediments (RUDD et al., 1986). Consequently, the high areal rates of SOD at station 4 do not contradict the low organic matter content. The low rates of P and N release also are a result of the abundance of allochthonous material at this site. This refractory organic matter is characterized by low N and P contents as evidenced by the relatively high C:N and C:P ratios (averages of 24.2 and 139, respectively). Bacteria degrading this organic matter must respire more carbon per unit of N or P released; consequently, the ratio of SOD to N release is 50% higher at station 4 than at stations 1 and 5.

The differences between stations 1 and 5 are more subtle, but they also may be important. The sediments at station 1 have a higher organic matter content probably as a result of higher rates of delivery of autochthonous material to this site. Station 1 sediments also have a lower C:N ratio indicating less extensive degradation of the organic matter at this site than at station 5. In contrast, station 1 has higher P release rates and lower P content than does station 5. The result is that the ratio of C:N:P release varies systematically with location in a lake or reservoir.

All diagenetic processes are driven by the input of organic matter. Spatial and temporal variability in sediment properties as well as in exchange rates are functions of

changes in the sedimentation flux. Decomposition of organic matter links the three processes of sedimentation, burial, and recycling. Hence, a model of decomposition kinetics is needed to predict rates of sediment-water exchange from sedimentation fluxes. Early diagenesis is a biologically mediated process. Oxidation of organic matter and regeneration of inorganic nutrients are generally attributed to sediment microbiota (CAPONE and KIENE, 1988). If organic substrate is a limiting factor for microbial growth, spatial heterogeneity of sediment properties and changes in organic matter input over time are likely to coincide with varying biomass pool sizes in space and time. A new mechanistic model of early diagenesis is developed in this study. The kinetic formulation of the model explicitly includes microbial biomass as a state variable, and decomposition rates are proportional to this pool size. The effects of varying microbial biomass on sediment nutrient release are explored and model predictions are compared to predictions using simple first-order kinetics.

The main part of this thesis is written as a manuscript to be submitted to the Journal of Environmental Quality. A short introduction to the new model, methods and results of sediment incubation experiments that were used to verify model predictions, and a discussion of the experiments and the model simulations are included in the article. Methods and results from the New Croton study are given in Appendix 1, followed by an in-depth explanation of the model framework including all differential equations and steady-state solutions (App. 2). The other appendices comprise the experimental protocols (App. 3), more detailed experimental results (App. 4), and Visual Basic program code for a two-layer sediment box model (App. 5).

2. Article

Abstract

Sediments in many lakes and reservoirs are characterized by spatial heterogeneity of their properties and highly variable inputs of organic matter on time scales ranging from days to decades. Predictions of sediment nutrient release rates as needed in many water quality models have to account for this variability in space and time. For this study, a new model of early diagenesis (BIOSED), which explicitly includes microbial biomass as a state variable, was developed. Model predictions of sediment C and N release are compared to the commonly used, first-order, multi-G model, and the effects of changes in microbial biomass on nutrient mineralization are examined. The new model leads to substantially different predictions of N release in sediments with low organic C content. Over short time periods microbial biomass dampens oscillations in N release rates and over longer periods of eutrophication, immobilization of N into microbial biomass is shown to reduce N mineralization. Model simulations also suggest that the microbial biomass pool size and the rate of organic matter decomposition are closely linked to substrate quality. Anaerobic incubation experiments were conducted to better understand the role of different substrates in nutrient recycling. Amendment of sediment with labile substrate (i.e., fresh algae, amino acids) is shown to be a useful method to assess organic matter quality in sediments. The fraction of organic C associated with labile substrate varied greatly among surface grab samples of lake sediments (2-10%). In contrast with other studies, organic N seemed to be readily accessible for microbial breakdown and primarily bound to labile material in all sediment samples.

Introduction

Decomposition of organic matter in sediments has important implications for surface water quality management and plays a key role in studying biogeochemical processes in lakes, reservoirs, and the oceans. Burial rates of organic matter in sediments are needed to balance global and local element cycles, and rates of nutrient mineralization have a major influence on the trophic status of lakes and reservoirs. Internal phosphorus loading resulting from sediment phosphorus release can account for up to 80% of total P inputs to some lakes (LARSEN et al., 1981). If external P loadings are reduced in an effort to restore surface water quality, lake recovery can be significantly retarded by persistently high sediment release rates (LARSEN et al., 1981; ROSSI and PREMAZZI, 1991; WELCH et al., 1986).

This study focuses on microbial decomposition of organic matter in lake sediments and the resultant mineralization of carbon and nitrogen. Phosphorus, although of considerable importance for water quality, is not explicitly considered. The plethora of geochemical processes involving phosphorus (e.g., FILIPPELLI and DELANEY, 1996) add another level of complexity to early diagenesis modeling that might obscure the dynamics of microbial decomposition of organic matter. The roles of N and P as essential nutrients for bacterial growth are comparable. Hence, most results of this study pertaining to nitrogen cycling are also applicable to phosphorus cycling.

The central process in early diagenesis is biologically mediated. Oxidation of organic matter and regeneration of inorganic nutrients are generally attributed to sediment microbiota (CAPONE and KIENE, 1988). Moreover, bacterial biomass itself can

account for a significant fraction of organic matter in surface sediments (~16%, GÄCHTER et al., 1988; ~10%, TÖRNBLOM and BOSTRÖM, 1995). As a result, bacteria act simultaneously as sinks and sources for organic substrates and for inorganic nutrients (e.g., NH_4^+ , TUPAS and KOIKE, 1990; 1991). Changes in microbial biomass are closely linked to changes in decomposition rates. Harvey et al. (1995) showed through a set of phytoplankton decomposition experiments that high metabolic activities of bacteria coincide with increases in biomass and greatest losses of particulate organic carbon. A stoichiometric balance between carbon and nitrogen uptake, as regulated by bacterial C:N ratios and growth efficiency, couples the two element cycles (GOLDMAN and DENNETT, 2000). Thus, nitrogen mineralization is a function of bacterial growth requirements and substrate availability.

The traditional approach in water quality modeling, however, does not take explicit account of bacterial biomass (THOMANN and MUELLER, 1987). Biomass concentrations are implicitly part of the reaction rate constant and are commonly assumed to be at steady-state. This simplification might be valid in unperturbed systems and for long-term studies where seasonal variations can be ignored. However, not much is known about the effects of microbial biomass on sediment nutrient release in dynamic systems. Changes in microbial biomass in sediments over several years or decades can be expected as a result of anthropogenic lake eutrophication and restoration. Short-term variations in bacterial concentrations can be triggered by seasonal variations in organic matter inputs (e.g., algal blooms, TÖRNBLOM and BOSTRÖM, 1995).

In contrast to water quality models, simulation models in soil science commonly include biomass as a separate pool; decomposition rates of any substrate are assumed to

be proportional to the growth rate of its decomposers (PARNAS, 1975). Mineralization and immobilization of soil nitrogen by microorganisms have been studied experimentally (e.g., PAUL and JUMA, 1981), and the experimental findings have been incorporated into numerous simulation models for the decomposition of soil organic matter (for review see, VAN VEEN et al., 1981).

For our study a new model of early diagenesis (BIOSED) was developed by combining the traditional multi-G model (WESTRICH and BERNER, 1984) with more mechanistic elements from soils models. The new model explicitly includes the effects of biomass on organic matter decomposition and nutrient immobilization and mineralization. Predictions of carbon and nitrogen release using the BIOSED model and the multi-G model are compared. These comparisons serve to determine in which situations the use of a more complex kinetic formulation is justified. Magnitudes of possible errors associated with the assumption of constant biomass pools are estimated. The commonly used spatial extrapolation of nutrient release rates from point measurements is considered in the context of spatially heterogeneous substrate qualities. Historic increases in sedimentation fluxes as can be found in many culturally eutrophied lakes and reservoirs and accompanying effects of changes in the microbial biomass pool on nitrogen mineralization are also examined. Seasonal variations in nutrient release rates are a concern in water quality management. The potential of sediment microbiota to attenuate peaks in release rates caused by varying inputs of organic matter is evaluated and quantified.

Changes in organic matter quality have been related to long-term and short-term dynamics of carbon and nutrients (e.g., BOSATTA and ÅGREN, 1991) and bacterial

nutrient mineralization rates were shown to be proportional to substrate quality. One possible explanation for this dependence is a thermodynamic interpretation of the theoretical concept of organic matter quality: the number of enzymatic steps required for complete mineralization of organic carbon to carbon dioxide defines quality (BOSATTA and ÅGREN, 1999). In our study anaerobic incubation experiments are used to better understand the effects of substrate quality on carbon and nitrogen release from sediments. A range of sediments and their respective mineralization rates are examined, and changes in mineralization rates induced by sediment amendments with glycine and fresh algae are used to estimate the relative abundance of labile substrate in the sediments. Differences in availability of carbon and nitrogen for microbial breakdown are determined by relating C and N release rates to sediment C and N contents.

Model Framework

Box-Models

In recent decades many different modeling frameworks for early diagenesis have been developed. The most common approach is based on one-dimensional partial differential equations including various diagenetic processes such as biochemical reactions, diffusion, advection, adsorption, burial, and compaction (BERNER, 1980; BOUDREAU, 1996). Concentration profiles of both solid species (e.g., organic matter, FeS, Fe(OH)₃, MnO) and dissolved species (e.g., O₂, NO₃⁻, SO₄²⁻, NH₄⁺, CH₄) are computed (e.g., BILLEN, 1982; HUNTER et al., 1998; KELLY-GERREYN et al., 1999; KLUMP and MARTENS, 1989; PARK and JAFFÉ, 1999; SOETAERT et al., 1996; VAN CAPPELLEN and YIFENG, 1996). Nutrient fluxes into the overlying water can then be calculated from

concentration gradients at the sediment surface using Fick's first law. The effects of bioturbation and bioirrigation on the transport of solid and dissolved species may also be included (e.g., BOUDREAU and MARINELLI, 1994; VAN CAPPELLEN and YIFENG, 1996).

Another type of model proposed by Di Toro (2001) represents the sediment as two layers: a thin, surface layer, and the underlying bulk sediment. The mathematical representation is based on mass balance equations, and nutrient fluxes can be computed using mass transfer coefficients. Diagenetic processes are driven by constant input of settling particles from the water column. Organic matter from this sedimentation flux is decomposed microbially, and any residual is buried in the underlying sediment. The output flux is modeled using a burial velocity. In the lower layer (Box 2), the direct input of settling particles is replaced by the burial flux of partly decomposed material from the surface layer (Box 1).

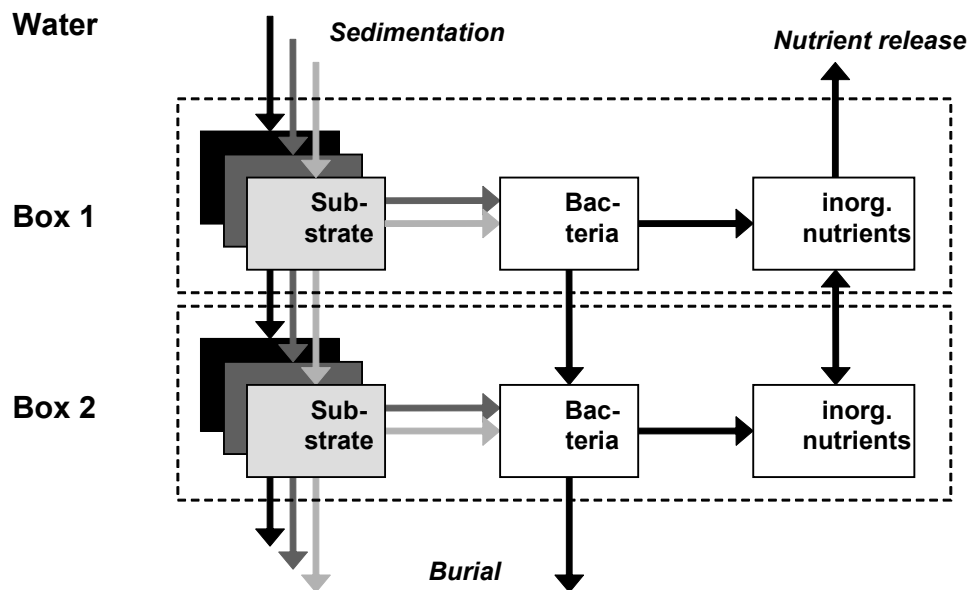


Figure 2-1 – Two-box model framework (shaded substrate boxes represent labile, stable, and refractory material)

This formulation can easily be integrated into comprehensive water quality models and simplifies investigation of different kinetic formulations for the prediction of sediment nutrient release. In this study a simple one-box model representing surface sediments is used for the majority of simulations. The relative importance of the surface layer is tested by including a second box (bulk sediment) and comparing contributions of the two boxes to the release of carbon and nitrogen.

Decomposition kinetics

Westrich and Berner (1984) have shown that decomposition of organic matter follows first-order kinetics and that the substrate pool can be divided into labile and stable fractions with significantly different reactivities and a refractory fraction that is not decomposed at all on a time scale relevant to water quality modeling. This framework is commonly referred to as the multi-G model. Mathematically, the total breakdown of organic substrate according to the multi-G model can be expressed as the sum of the breakdown of the three individual fractions,

$$rxn_l = k_l \cdot C_l \quad (1)$$

$$rxn_s = k_s \cdot C_s \quad (2)$$

$$rxn_r = 0 \quad (3)$$

where rxn stands for changes in labile (l), stable (s), and refractory (r) substrate due to decomposition reactions, k_l and k_s are first-order rate constants, and C_l and C_s are the labile and stable substrate concentrations.

The model presented in this study (BIOSED) combines the multi-G model with more mechanistic elements as can be found in soil models. Microbial biomass is explicitly included as two state variables (microbial C, microbial N), and the kinetic formulation is based on five main assumptions:

- 1) The rate of organic matter breakdown is proportional to the concentration of decomposers in the system;
- 2) Organic matter is subdivided into labile, stable, and refractory substrate pools according to the multi-G model;
- 3) A constant microbial efficiency determines the fraction of substrate carbon respired;
- 4) Carbon and nitrogen cycles are coupled using fixed but distinct C:N ratios for all substrate pools and the biomass pool;
- 5) The size of the biomass pool is limited by a constant “recycling rate” that integrates such factors as competition, death, and predation.

Mathematically, the dependence of the decomposition kinetics on microbial biomass is included by introducing a dimensionless biomass concentration C_b/C_{b0} (i.e., proportionality factor). A dimensionless factor simplifies the comparison of the two models, since identical rate constants can be used in both frameworks. The change in microbial biomass follows

$$\frac{dC_b}{dt} = \frac{C_b}{C_{b0}} \cdot (k_l \cdot C_l + k_s \cdot C_s) - r \cdot C_b \quad (4)$$

where C_b is the biomass carbon concentration, C_{b0} is the biomass normalization factor, k_l and k_s are first-order rate constants, C_l and C_s are labile and stable substrate C concentrations, and r is a constant microbial death rate. Bacteria require carbon substrate

for their assimilatory and dissimilatory metabolism and therefore have to decompose more substrate than the amount taken up for cell growth. In microbial ecology this is commonly expressed as a constant growth yield or C uptake efficiency. Thus, substrate breakdown follows

$$rxn = \frac{1}{eff} \cdot \frac{C_b}{C_{b0}} k \cdot C \quad (5)$$

where *rxn* stands for change in substrate (labile or stable) due to decomposition reactions, and *eff* is carbon uptake efficiency.

To allow comparison of the BIOSSED model and the multi-G model, a reference scenario was chosen, in which steady-state rates of organic matter breakdown in both models are set to be equal. Thus, in the reference scenario

$$\frac{1}{eff} \cdot \frac{C_b}{C_{b0}} = 1 \quad (6)$$

Deviations from the reference scenario are then used to determine the effects of various parameters and environmental variables on the multi-G model and the BIOSSED model.

Whether bacteria are limited by the availability of substrate carbon or substrate nitrogen depends on the overall C:N ratio of the decomposable organic matter, the microbial C:N ratio, and microbial C assimilation efficiency (PARNAS, 1975). Assuming a nitrogen uptake efficiency of one, carbon limitation occurs when

$$C : N_{substrate} < \frac{C : N_{biomass}}{efficiency} \quad (7)$$

In the literature on sediment processes, no evidence for nitrogen-limited growth of bacteria was found. A rough estimation based on typical values for microbial C:N ratios and efficiencies also suggests that nitrogen limitation will not occur in most lacustrine

systems if bacterial C efficiencies are <25%. Therefore, nitrogen pool sizes and breakdown are determined by the corresponding carbon pools and rates:

$$\frac{dNitrogen}{dt} = \frac{1}{C:N} \cdot \frac{dCarbon}{dt} \quad (8)$$

Methods

Anaerobic incubation experiments with sediment slurries from four different locations were conducted over a time period of 21 days to assess the effects of substrate quality on C and N release rates. Release rates were assessed by measuring DIC and dissolved and sorbed ammonium in the slurries after successive time intervals. Sediment properties including porosity, solids concentration, loss-on-ignition (LOI), and C and N content were measured to characterize substrate quality. Additional incubation experiments using sediments amended with glycine and fresh algae were performed to evaluate the response of C and N release to additions of labile substrate with different C:N ratios.

Sediment collection

Grab samples of surficial sediments were collected with an Ekman dredge at four locations on the Keweenaw Peninsula, Upper Michigan. The sampling sites reflect a range of sediment properties as shown in Table 2-1. Dollar Bay (DB) and Chassell Bay (CB) are mesotrophic to eutrophic embayments of Portage Lake. Lily Pond (LP) is a shallow pond (<1.5m) near the North Entry of Portage Canal that receives significant amounts of plant detritus from macrophytes and the surrounding wetland vegetation. Sediments at the Sturgeon Sloughs site (SS) are low in organic matter content and are

strongly influenced by material transported from upstream Sturgeon River and surrounding marsh lands. Sediment from Dollar Bay, Lily Pond and Sturgeon Sloughs were sieved (1 mm mesh size) to remove coarse material. All samples were stored in the dark at 4°C and covered with hypolimnetic water.

Anaerobic incubations

All sediment samples were amended with excess nitrate to inhibit methanogens (KRISTENSEN and HOLMER, 2001; LOVLEY and KLUG, 1986; LOVLEY and PHILLIPS, 1987). Thus, changes in total dissolved inorganic C concentrations represent total C release, and methane evolution does not have to be monitored. The stoichiometry of denitrification is $4 \text{ NO}_3^- + 5 \text{ CH}_2\text{O} \rightarrow 5 \text{ HCO}_3^- + 2 \text{ N}_2 + 2 \text{ H}_2\text{O} + \text{ H}^+$. The amount of nitrate needed to completely decompose 70% of all organic C (i.e., 30% is assumed to be refractory C) was calculated from organic C content for each sediment. Organic C was estimated from solids concentration and loss-on-ignition data (Table 2-1). To allow the microbial pool to adapt to the incubation temperature and the nitrate addition, the amended sediments were preincubated for 2 days in the dark at 20°C. At the start of the actual incubation period, the sediment was diluted and homogenized prior to transfer to 50-mL screwcap glass vials. Dilution rates were adjusted for the four sediments such that centrifugation of the slurry yielded a supernatant volume of 15-25 mL. Nine replicates per sediment type and treatment were incubated in a tumbler at 20°C.

Only Dollar Bay sediments were used for substrate addition experiments. Substrate was added at the beginning of the incubation period, all other steps were similar to the unamended samples to ensure comparability of the results. One set of samples received ~1.6 g/L additional organic carbon by adding the green algae *Selenastrum capricornutum*

(DBA). Two sets were amended with the amino acid, Glycine, in amounts of ~ 2.4 g C/L (large addition, DBLG) and 1.2 g C/L (small addition, DBSG), respectively.

The first measurements were made after 21 hrs and then weekly thereafter. On each day of sampling, one to three vials per treatment were removed from the tumbler and pre-processed for the analytical measurements. To avoid air contact of the samples, pH was measured in a glass flow-through cell (800 μ L) with a microtip Ag/AgCl combination electrode. About 5 mL of sediment slurry was displaced from the vial into the cell through the vial septum by injecting nitrogen gas into the incubation vial. To complex reduced iron species, 1 mL of 7.5% EDTA solution was then injected with a syringe. Experimental test runs had shown that formation of iron hydroxides occurred very rapidly in all DB, CB and SS samples upon exposure to air and resulted in significant drops in pH. The interstitial water was separated from the solid fraction by centrifugation (1900 rpm, 25 mins), and 0.5 - 1.0 mL of supernatant was withdrawn and frozen for ammonium measurements. The remaining supernatant was decanted into 50-mL beakers, weighed, and analyzed for total carbonate alkalinity on the same day. The solid fraction was frozen and stored until further analysis.

Analyses

All four sediment samples were analyzed for water content and solids concentration by drying a known volume at 70°C for 24 hrs. Organic matter content was estimated by determining the loss-on-ignition. Dried samples were combusted at 550°C following the method of Dean (DEAN, 1974). Standard deviations for water content and loss-on-ignition measurements were $\pm 0.9\%$ and $\pm 0.4\%$ respectively. An Elemental Analyzer (Fisons NA1500 NC) was used to measure sedimentary C and N contents. Standard deviations as

determined from replicate measurements were $\pm 15.0\%$ for C analysis and $\pm 11.6\%$ for N analysis.

Total dissolved inorganic carbon was calculated from the pH values measured in the flow-through cell and total carbonate alkalinity. To determine alkalinity the supernatant was titrated with standardized acid (0.1 N HCl) to $\text{pH} < 4.5$ (CLESCERI et al., 1998). Recovery of total dissolved inorganic carbon using the combined pH and alkalinity measurements was over 97%.

Dissolved ammonia in the interstitial water was measured according to the standard phenate method (CLESCERI et al., 1998; SOLORZANO, 1969). The standard deviation of replicate measurements was $\pm 3.5\%$. Adsorbed ammonium was extracted by resuspending a representative subsample of the solids in 1N KCl and shaking for one hour (MACKIN and ALLER, 1984). No centrifugation was necessary to separate the solids from the liquid phase and the concentrations were determined by the phenate method. The standard deviation for the ammonium extraction was $\pm 13.5\%$.

Model simulations

Analytical solutions for steady-state scenarios can be derived for the multi-G and the BIOSSED model. To evaluate differences in predictions of C and N release between the two models, steady-state concentrations and C and N fluxes were calculated for different scenarios. The results are used to examine model behavior over a wide range of substrates and to elucidate the effects of varying model parameters.

Time-dependent simulations were solved numerically using a first-order forward Euler method; both models were implemented as Excel[®] macros (Visual Basic for Applications). Two nonsteady-state scenarios were simulated to examine differences in

model behavior. The objective of the study was not to mimic reality, but to show possible shortcomings of the commonly used multi-G model in simplified but reasonable situations. The first scenario simulates the effects of prolonged eutrophication over 10 years. Eutrophication is represented as a linear increase in organic matter input (10% pa.). This increased carbon flux is obtained by increasing the sedimentation flux continually from $\sim 0.15 \text{ g cm}^{-2} \text{ yr}^{-1}$ to $\sim 0.17 \text{ g cm}^{-2} \text{ yr}^{-1}$ and the organic matter content of the settling particles from 11.4% to 25%. Stable material does not contribute to the increase in organic matter and refractory material is assumed to be a constant fraction of settling material (25 % of org. C). Therefore, the fraction of labile material increases from 50% to 65% of settling organic carbon over the simulation period.

The second scenario represents the effects of seasonal variations in organic matter inputs. Short-term peaks in organic matter inputs occur in many lakes, reservoirs and the oceans due to algal blooms. Nutrient release is modeled over a one-year-period. The steady-state concentration of organic C in settling particles is 5%; between day 120 and 160 this value rapidly increases over ten days to a maximum concentration of 15%, remains at this value for 20 days, and is reduced to its original value over another 10 days.

Results

Sediment C and N contents

Due to the geological setting of the area, carbonate was assumed to be absent from all sediments. Good correlation between loss-on-ignition and elemental analysis results supports this assumption. Carbon content ranges from ~1.8% in the organic-poor Sturgeon Sloughs sediments to ~15.5% in the Dollar Bay sediments. Both Lily Pond and Chassell Bay have intermediate carbon contents of ~5%. C:N ratios (molar basis) of all sediment types are relatively high and indicate significant input of terrestrial material into all four systems. Sturgeon Sloughs sediments have the highest molar C:N ratio (~18.3) followed by Dollar Bay (~18.0) and Lily Pond (~17.8). Chassell Bay exhibits a slightly lower value (~16.0). Properties of unamended sediments are summarized in Table 2-1.

Carbon and nitrogen contents of algae-amended sediments were 6.9% and 8.4% higher than in the unaltered sediment (Table 2-1); the overall C:N ratio decreased only slightly. Glycine ($C_2H_5NO_2$) additions significantly altered the sediment composition. Changes in carbon content were on the same order of magnitude as in the algae-amended sediments (DBLG: +9.0%, DBSG: +5.8%). Nitrogen content, however, was almost doubled by the large glycine addition (+81.4%). The small glycine addition caused an increase in sediment N of 52.6% (Table 2-1).

**Table 2-1 – Properties of unamended and amended sediments
(analytical errors are given in the text)**

Sediment	Porosity (%)	Bulk density (g cm⁻³)	Loss-on- Ignition (%)	C content (%)	N content (%)	C:N ratio (molar)
Dollar Bay	90.6	0.96	28.5	15.5	1.00	18.1
Chassell Bay	75.8	1.10	14.3	4.8	0.35	16.0
Lily Pond	69.1	1.11	8.6	4.6	0.30	17.8
Sturgeon Sloughs	46.2	1.53	3.8	1.8	0.12	18.3
Dollar Bay + Algae	-	-	-	16.6	1.09	15.3
Dollar Bay + lg. Glycine	-	-	-	16.9	1.82	9.3
Dollar Bay + sm. Glycine	-	-	-	16.4	1.53	10.7

Incubation experiments

Despite the variability in sediment C content, only small differences in carbon release rates were observed among sediment types. The addition of labile substrate (i.e., glycine and fresh algae) resulted in higher decomposition rates and increased carbon release. Nitrogen release rates differed significantly among sediment types and amendments. Nitrogen release from Dollar Bay sediments exceeded release from any other unamended sample by more than twofold. Comparable amounts of nitrogen were released from Chassell Bay and Lily Pond samples. Sturgeon Sloughs showed the lowest rate. Dollar Bay sediments amended with nitrogen-rich glycine exhibited increased nitrogen release. Despite the strong increase in carbon release rate from algae-amended sediments, nitrogen release from this set of samples was only slightly higher than in the control. Table 2-2 and Table 2-3 show carbon and nitrogen release rates for all unamended and amended sediments.

Table 2-2 – Carbon release rates (per sediment dry weight)

Sediment	C release rate ($\mu\text{mol g}^{-1} \text{d}^{-1}$)	Standard error ($\mu\text{mol g}^{-1} \text{d}^{-1}$)	R ²	n
Dollar Bay Control	0.50	0.27	0.539	3
Chassell Bay	0.83	0.097	0.987	3
Lily Pond	0.80	0.48	0.586	4
Sturgeon Sloughs	0.35	0.091	0.936	3
Dollar Bay + Algae	2.4	0.12	0.998	3
Dollar Bay + lg. Glycine	1.3	0.58	0.831	3
Dollar Bay + sm. Glycine	2.0	0.24	0.959	3

Table 2-3 – Nitrogen release rates (per sediment dry weight)

Sediment	N release rate ($\mu\text{mol g}^{-1} \text{d}^{-1}$)	Standard error ($\mu\text{mol g}^{-1} \text{d}^{-1}$)	R ²	n
Dollar Bay Control	0.56	0.059	0.953	3
Chassell Bay	0.17	0.062	0.783	3
Lily Pond	0.22	0.073	0.817	4
Sturgeon Sloughs	0.071	0.009	0.992	3
Dollar Bay + Algae	0.9	0.11	0.722	3
Dollar Bay + lg. Glycine	1.6	0.35	0.908	3
Dollar Bay + sm. Glycine	1.6	0.10	0.984	3

Carbon and nitrogen release rates normalized to sediment C and N content are good measures of the abundance of labile substrate. These values correspond to the percentage of available C or N being broken down per day (Figure 2-2). The fraction of organic carbon decomposed per day is similar in Chassell Bay, Lily Pond, and Sturgeon Sloughs sediments. Dollar Bay sediments behave differently: either the overall rate of organic matter breakdown is significantly lower than in all other systems, or a larger fraction of available organic carbon is refractory material. N release follows similar patterns at all sites (Figure 2-3). The carbon utilization rate (i.e., percentage of org. C released as DIC

per day) increased by a factor ~4.5 due to the addition of algae and by a factor ~3.8 for the small glycine addition (Figure 2-2). Nitrogen utilization was similar in the control and the algae-amended samples and enhanced in glycine-amended sediments. (Figure 2-3).

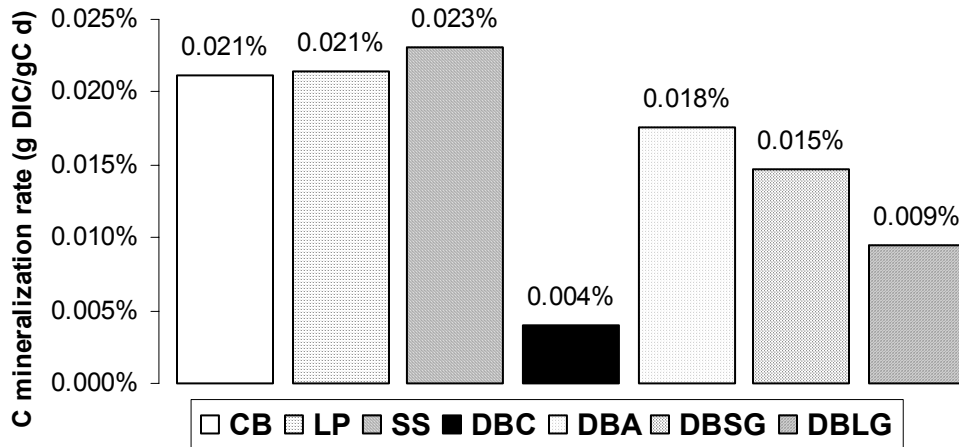


Figure 2-2 – All sediments: Percentage of sediment C released as DIC per day

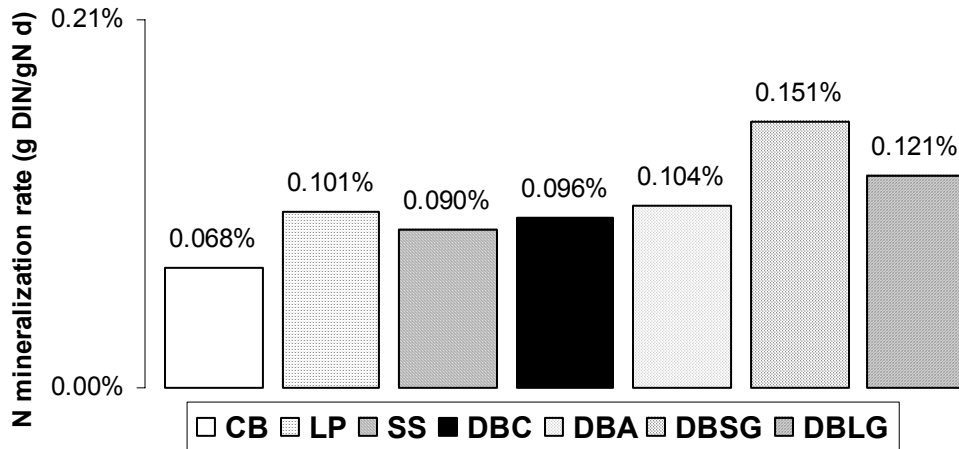


Figure 2-3 – All sediments: Percentage of sediment N released as DIN per day

Steady-state

Analytical solutions to the multi-G and the BIOSED model were used to compare model responses to changes of three parameters: microbial C uptake efficiency, sedimentation flux, and fraction of labile substrate. Microbial respiration and growth in the BIOSED model are dependent upon a user-specified C uptake efficiency. Figure 2-4 shows the effect of varying efficiency on the fraction of microbial biomass in the surface sediment. Nitrogen release also varies with microbial efficiency. Models excluding microbial biomass are not able to capture this variability. Changes in efficiency within a realistic range cause deviations from the N release rate in the reference scenario of 10 – 15% (Figure 2-5).

Sedimentation fluxes of organic carbon are closely linked to trophic status and range over three orders of magnitude (TARTARI and BIASCI, 1997). Both models predict a linear correlation of N and C mineralization rates with the rate of settling organic matter (Figures not shown). At low inputs, however, the BIOSED and multi-G model differ by more than 25% in the prediction of N mineralization (Figure 2-6).

Variations in the ratio of labile to stable organic matter in the sedimentation flux result in variations in sediment C:N ratios. High inputs of labile (autochthonous) substrate lead to lower overall C:N ratios, whereas sediment dominated by stable (allochthonous) substrate has a higher C:N ratio. Both models show similar C:N ratios of mineralized products for sediment C:N ratios of 14 to ~20. The ratio of carbon to nitrogen release increases from ~6.5 to ~9.1 in this range. For higher values of sediment C:N ratios model predictions diverge markedly (Figure 2-7).

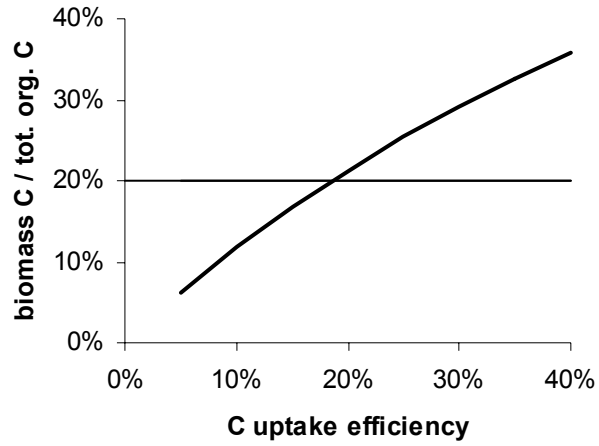


Figure 2-4 – Model: Effect of varying C uptake efficiency on biomass pool size

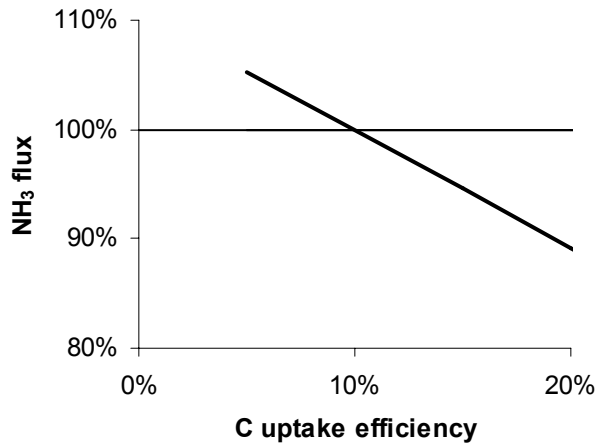


Figure 2-5 – Model: Effect of varying C uptake efficiency on N release rate (normalized to reference scenario)

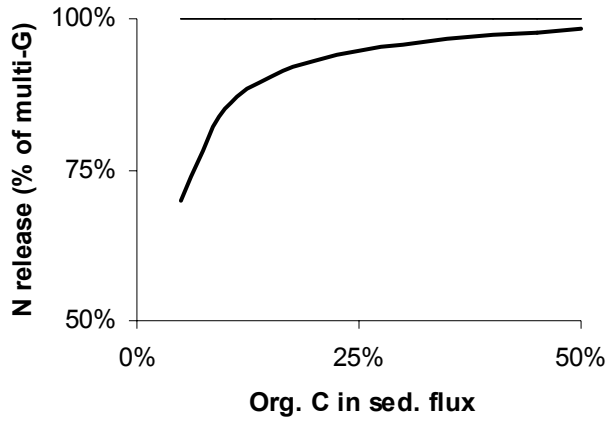


Figure 2-6 – Model differences in N release rates as a function of organic matter input (BIOSED normalized to multi-G)

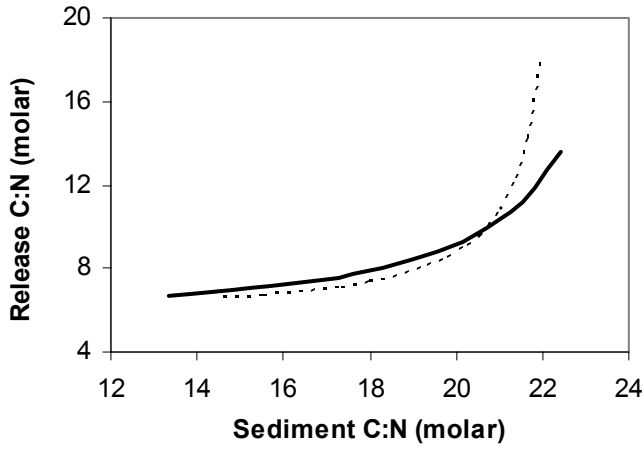


Figure 2-7 – Model: Effect of sediment C:N ratio on release C:N ratio (- - - multi-G, — BIOSED)

Time-dependent simulations

In the first nonsteady-state scenario (i.e., prolonged eutrophication), both models show linear increases in C and N release with increasing organic matter input. The biomass pool, growing from initially ~8% of organic C in the surface sediment to ~15% at the end of the 10 year period, is also linearly correlated to the sedimentation flux. Biomass growth requires nutrients that are immobilized from the substrate. This process is not included in the multi-G model and causes differences between the models in predicted C and N mineralization rates (Figure 2-8).

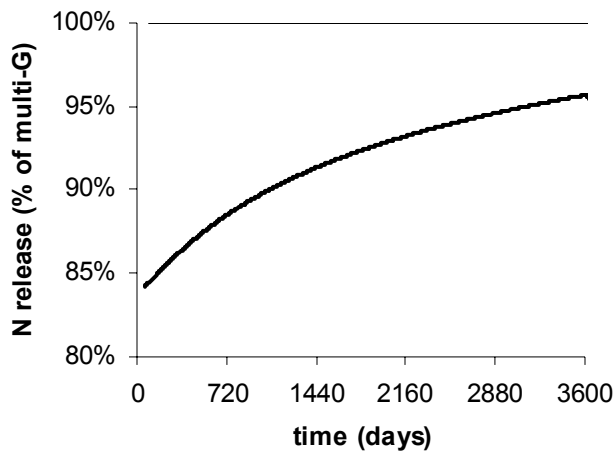


Figure 2-8 – Model: Long-term eutrophication: Differences in N release (BIOSED normalized to multi-G)

Both models respond to a seasonal peak in organic matter input (second scenario) with enhanced N release and return back to the steady-state release rate after the end of the pulse (Figure 2-9). Cumulative amounts of additional N release due to the sedimentation peak (areas under the curves) are equal and show the validity of the mass balance in both models. The temporal pattern of the two model responses, however, is markedly different. Growth and decline of biomass in the BIOSED model act as a buffer for nutrient release and prolong the time period affected by the sedimentation event while

reducing peak release rates. Excluding biomass from the decomposition model can therefore lead to overpredictions of the maximum N release rate of more than 70%. These overpredictions in maximum release rates are coupled to underpredictions of the duration of increased N release. The multi-G model returns to steady-state approximately 60 days after the end of the pulse, whereas the BIOSED model shows enhanced N release rates for more than 200 days.

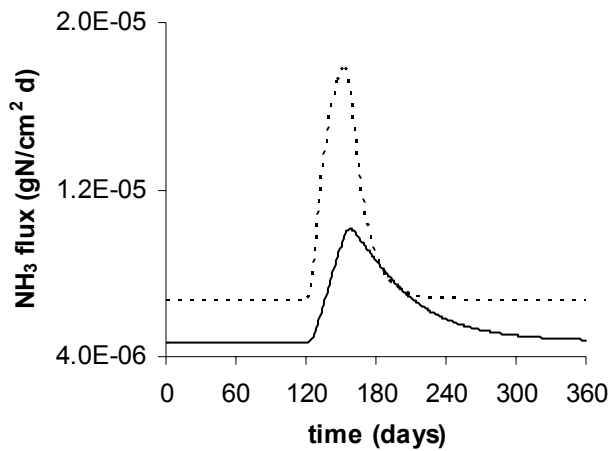


Figure 2-9 – Model: Short-term sedimentation event (algae bloom): N release rate (- - - multi-G, — BIOSED)

Two-Box model

The importance of decomposition processes at the sediment surface was examined by comparing the relative contribution of the surface layer and the bulk sediment to total C and N release. Residence times in the two boxes are 150 days in the top layer and 3000 days in the bottom layer corresponding to layer thicknesses of 0.3 cm and 6 cm, respectively. Organic matter degradation follows the same kinetics in both boxes and mass balance of solid and dissolved species is assured through burial fluxes and mass transfer (diffusion). Figure 2-10 shows that according to the BIOSED model ~90% of all labile material and ~35% of the stable material is decomposed in surficial sediments. The

multi-G model predicts similar values (not shown). Due to its lower C:N ratio, breakdown of labile organic matter contributes the majority of released N. It is therefore not surprising that the bulk sediment (Box 2) only accounts for ~1% of total nitrogen released. In the BIOSSED model, differences in substrate availability between the two boxes are also reflected in respective biomass pool sizes (Box 1: 1.6 mg C/cm³, Box 2: 0.6 mg C/cm³). Aller and Yingst (1980) showed that direct counts of bacterial numbers decrease by a factor of 2-3 over the top 10 cm of marine sediment. Similar patterns were also observed in sediments of eutrophic (Lake Erie, MATISOFF et al., 1981) and hypereutrophic (Lake Sempach, GÄCHTER et al., 1988) lakes.

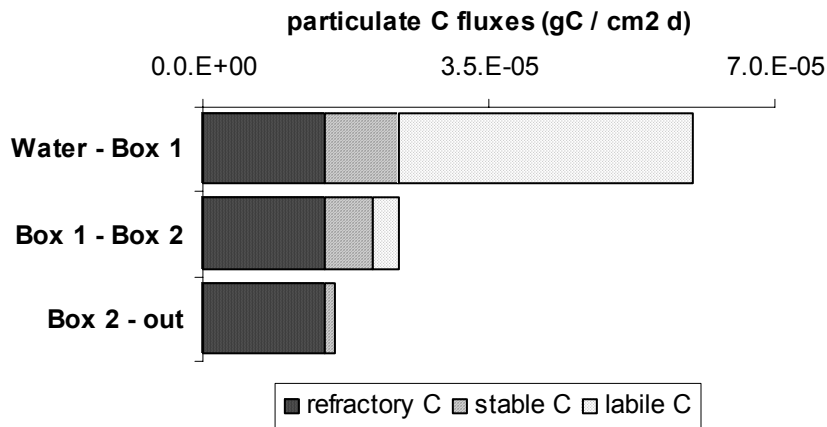


Figure 2-10 – Two-Box BIOSSED model: POC fluxes between water and sediment, between boxes, and burial flux.

Discussion

Substrate Quality

Abundance and quality of the organic matter in sediments strongly influence the rates of C and N release. Analytical solutions to both models predict a linear increase of C and N release with increasing input of organic matter. Different reactivities of substrate fractions as expressed by different rate constants and distinct C:N ratios of the substrate pools, however, complicate the relationship between sediment properties and C and N mineralization. Sediments receiving high inputs of labile, nitrogen-rich substrate (e.g., phytoplankton) show patterns of C and N release that differ from sediments dominated by more stable, nitrogen-poor material (e.g., terrestrial material). Both models capture the variability of C and N release rates with varying organic matter quality, but the model predictions diverge for sediments rich in stable material (Figure 2-7). Experimental results can help to understand the effects of substrate quality on decomposition kinetics. Estimates of labile, stable, and refractory substrate pool sizes are needed for models of early diagenesis. Long-term incubation experiments can be conducted to determine the different organic matter fractions (e.g., WESTRICH and BERNER, 1984), but short-term incubations and sediment amendment experiments also yield valuable information on substrate quality.

The relationships between sediment properties and mineralization rates are markedly different for carbon and nitrogen. Nitrogen release is linearly correlated with the nitrogen content of the sediments (Figure 2-11). The more organic nitrogen is available, the more is mineralized and released. An analogous simple relationship is not

found for carbon release. This can be the result of different availabilities of particulate organic carbon (POC) and particulate organic nitrogen (PON) to microbial metabolism in sediments. The similar percentage (0.07-0.1%) of N release per day among unamended sediments (Figure 2-3) suggests that organic nitrogen is equally accessible to bacteria in all four types of sediment. Nitrogen utilization rates in amended versus unamended Dollar Bay sediments support the assumption that most nitrogen is bound to easily decomposable material (Figure 2-3). The percentages of nitrogen released per day are similar for the control (0.096%) and the algae amendment (0.104%). The increase in the fraction of N (to 0.15% per day) that is mineralized in glycine-amended sediments (small addition) reflects the large excess of nitrogen being added to the sediments, but the increase is lower than what might be expected from the enhanced carbon utilization rate and the substrate C:N ratio (Glycine: molar C:N = 2). Microbial cometabolism of amino acids and NH_3 (GOLDMAN and DENNETT, 2000) might obscure N mineralization in the glycine-amended sediments. The correlation of N release with N content that was found for all unamended samples and the similarity in N utilization in algae-amended Dollar Bay sediments and the control suggest that most organic N is in a labile pool.

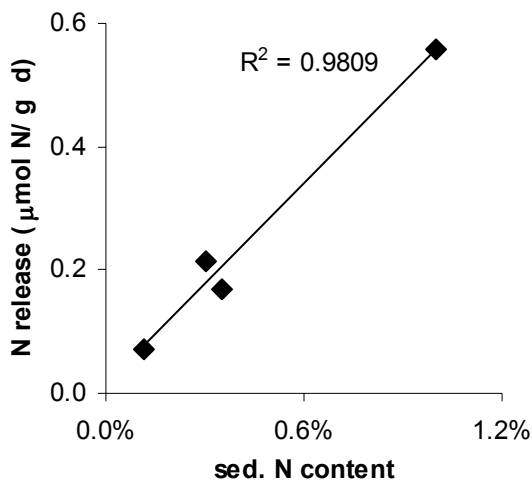


Figure 2-11 – Unamended sediments: N release rates vs. sediment N content

The distribution of organic carbon among reactive and non-reactive substrate pools on the other hand, appears to differ among the four sites. The fraction of labile substrate at the four sites can be estimated from differences in the percentage of organic C released among the four unamended sediments and comparison of unamended and algae-amended Dollar Bay sediments (Figure 2-2, Figure 2-12). Since carbon release is dominated by labile carbon decomposition, the change in carbon utilization due to the algal addition is proportional to the change in the labile pool. Assuming that added algal biomass contributes in its entirety to the labile pool, the initial pool of labile material can be calculated from the increase in carbon content due to the addition of algal biomass and the increase in daily carbon utilization.

Our data suggests that labile material contributes only ~2% to the total organic carbon pool in unamended Dollar Bay sediments. Labile organic carbon in Chassell Bay, Lily Pond, and Sturgeon Sloughs sediments is estimated to account for ~10% of total organic carbon. Explanations for the different behavior of Dollar Bay sediments include the observation of large amounts of woody debris and the possible collection of deeper, more decomposed material due to the high porosity of the sediments. Extended periods of anoxia in Dollar Bay (URBAN, personal comment) may also have an effect on the degradability of organic matter. Comparisons of oxic and anoxic decomposition experiments have shown that the amount of undegradable organic matter is about twice as high under anoxic conditions (LEHMANN et al., 2002). Although much remains unknown about the factors influencing organic matter quality, sediment amendment experiments are a valuable tool for the estimation of both the fraction of labile material and its decomposition rate.

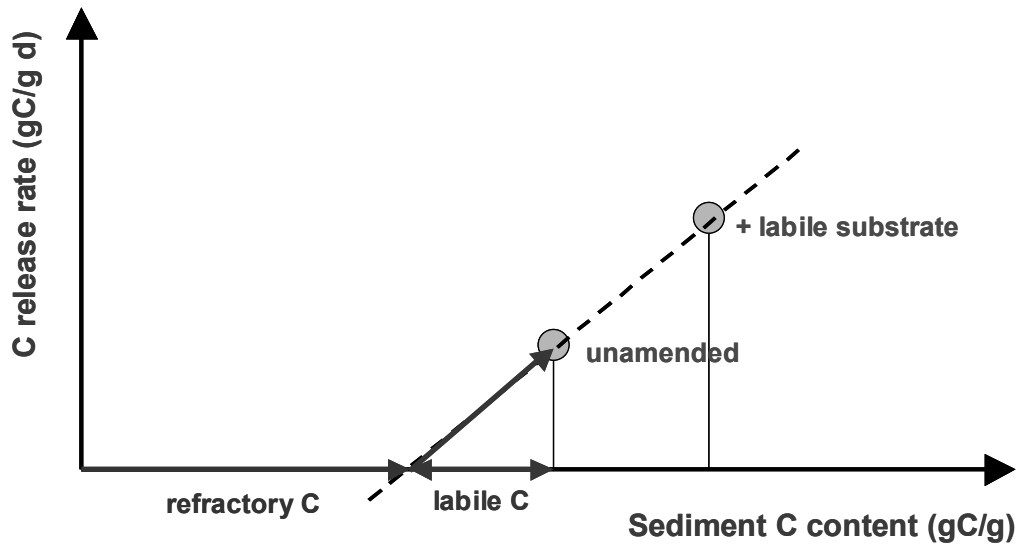


Figure 2-12 – Estimation of the labile C pool using sediment amendment experiments. Changes in C release rates due to the addition of labile substrate (e.g., fresh algae) are used to estimate the initial fraction of labile C in the unamended sediments (assumptions are stated in the text)

Biomass pool size

In the multi-G model, decomposition rates are independent of microbial biomass. Carbon and nitrogen release rates only vary as a function of the relative abundance of labile and stable organic matter and the respective C:N ratios of those fractions. In the BIOSSED model, decomposition rates are proportional to the size of the biomass pool. Thus, variations in microbial biomass due to variations in organic matter inputs have an immediate effect on C and N mineralization rates (Figure 2-13). The multi-G model implicitly assumes a constant biomass pool across a range of sediment organic matter contents and sediment C:N ratios. As a result, decomposition rates and thus predictions of N release rates are higher in the multi-G model than in the BIOSSED model for organic matter-poor sediments or for sediments with a high proportion of stable material (Figure 2-6).

The BIOSSED model illustrates that it is the interaction of microbial growth efficiency, and growth and death constants that constrain the magnitude of the microbial biomass in sediments. According to studies by Törnblom and Boström (1995) and Gächter (1988) biomass pools in the surface sediments of eutrophic lakes account for 10-16% of sedimentary organic carbon. Microbial counts revealed a relative constancy of microbial pools across a wide range of marine sediments (SCHMIDT et al., 1998). These studies suggest that the biomass pool in sediments may be limited by factors such as competition, predation, and growth limitation by nutrients or electron acceptors; literature on these factors is scarce. The BIOSSED model predicts that the pool of microbial biomass will increase as the growth efficiency increases (all other factors remaining constant). According to the BIOSSED model, the pool sizes that are reported in the scant literature on the subject can only exist if growth efficiencies are less than 20% (given a ratio of microbial death to growth rate constants of 10); higher growth efficiencies would need to be coupled with higher microbial death rates. Clearly, more work is required to determine the factors controlling biomass growth and turnover in sediments. However, the complex interdependency of microbial growth rate, death rate, efficiency, and decomposition of organic matter in sediments is reflected on a conceptual level in the BIOSSED model.

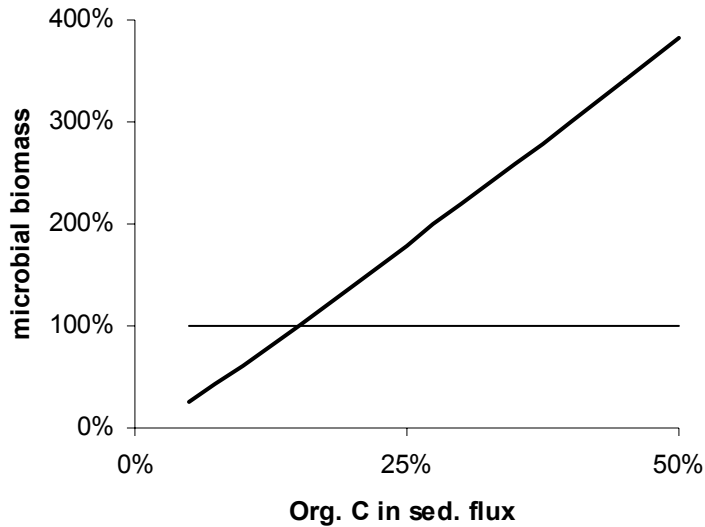


Figure 2-13 – BIOSED: Change in microbial biomass with varying organic matter input (normalized to reference scenario)

Although not much is known about microbial growth and turnover in sediments, time-dependent model simulations show clearly the importance of these processes for the prediction of sediment N release. Increases in organic matter inputs are coupled to an increase in microbial biomass (Figure 2-13). Bacterial growth requires nutrients, which are immobilized from the substrate pool instead of being mineralized as inorganic nutrients. Models that assume a constant biomass pool therefore overpredict N release rates if biomass growth is occurring. For a continuous increase in organic matter input (prolonged eutrophication), the reduction of mineralization rates due to microbial nutrient immobilization continues until a maximum biomass pool size is reached. Further increases result either in higher turnover rates or increased burial of undecomposed organic matter. More specifically, the BIOSED model results suggest that over a time period of 10 years biomass growth can account for immobilization of as much as 10% of the nitrogen gained from organic matter breakdown (Figure 2-8).

For short-term peaks in organic matter inputs, immobilization decreases the rate at which nutrient mineralization responds to the higher input. Death and recycling of biomass into the substrate pool as a consequence of reductions in organic matter loadings increase nutrient release rates until the system returns to steady-state (Figure 2-9).

Water quality modeling

The implications of the model comparisons for water quality modeling are twofold. First, the dependency of the microbial biomass pool size and thus of the decomposition rates on organic matter content and substrate quality can be a concern in spatially heterogeneous systems, if kinetic rate constants are extrapolated from point measurements. Model comparisons show a clear divergence for organic matter-poor sediments (Figure 2-6) and sediments dominated by allochthonous (stable) material (Figure 2-7). The use of invariant decomposition rates for a range of sediment properties as can be found in many lakes and reservoirs does not reflect changes in decomposition kinetics that are caused by variations in the size of the biomass pool. It is therefore not only desirable to incorporate into a model of early diagenesis the heterogeneous, spatial distribution of sediment properties, but also the resultant heterogeneity in microbial pool sizes and decomposition rates.

Second, the multi-G model also misrepresents the temporal dynamics of nutrient release. Mineralization rates are directly influenced by nutrient immobilization into microbial biomass, and increased biomass pool sizes are coupled to increased decomposition rates. In the eutrophication scenario, the assumption of constant biomass predicts nutrient release rates that are more than 10% higher than with a variable biomass pool (Figure 2-8). The two microbial processes that influence nutrient mineralization

rates, immobilization and changing decomposition rates, are likely to counterbalance each other to a certain extent. While the absolute concentration of biomass C in sediments more than doubles with a doubling of organic matter inputs (Figure 2-13), model predictions of N release only differ by slightly more than 10% in the eutrophication scenario (10% increase in org. C per year over 10 years). The increase in the rate of organic matter decomposition (proportional to the absolute biomass pool size) is outweighed by the growth requirement of the microbes and the resultant nutrient immobilization.

Incorporation of microbial biomass into the decomposition model also has implications for seasonal variations in organic matter input. Predictions of C and N fluxes in response to a spike of organic matter input (i.e., algal bloom) suggest that biomass growth and turnover are able to attenuate peaks in nutrient release (Figure 2-9). Increased N immobilization due to biomass growth reduces the maximum N release rate. Increased decomposition rates and recycling of biomass into the substrate pool prolong the duration of higher N release rates. Comprehensive surface water quality models that are used to determine reservoir management decisions on a daily or weekly basis will respond differently to the prediction of N release from a multi-G sediment model versus the BIOSSED model. The cumulative N release is independent of the incorporation of biomass into the sediment decomposition model. Hence, a long-term N mass balance on the lake might not be influenced by the predicted differences in N release over time. This illustrates how the choice of a more mechanistic model versus a simpler first-order model depends on its intended application. Nitrogen immobilization into microbial biomass can account for a significant fraction of decomposed organic nitrogen, and decomposition

rates are likely to vary with changes in the microbial pool size. Models that do not explicitly include effects of microbial growth and turnover on nutrient immobilization and mineralization are not able to fully capture the variability in nutrient release in nonsteady-state situations.

3. Appendices

Appendix 1: Croton Watershed sediments

Within the context of the Croton Watershed study, sediments were studied for three reasons. First, sediments were collected to map the distribution of physical and chemical parameters (e.g., phosphorus and iron content) that may feed into water quality models. The depth distribution of these parameters gives insight into how management practices have influenced sediment properties. These results are presented in section A below. Second, the sediments were studied to determine rates of biogeochemical processes (nutrient release); these rates are incorporated directly into the water quality models. These studies are documented below in section B. Finally, the sediment stratigraphy was studied to refine a model of sediment diagenesis. In the future, this model will be incorporated as a component of the overall water quality model. First, however, additional studies are needed to clarify the spatial variability in sediment processes.

A) Stratigraphy of New Croton Reservoir Sediments

Methods and Materials

Multiple sediment cores were obtained from the Croton Reservoirs between 9 August and 13 August 2000. In New Croton Reservoir, sediment cores were taken from stations 1, 4 and 5. Station 8 was too sandy to allow retrieval of an intact core. A Jenkins corer was used to obtain sediment cores of 20-40 cm in length; only cores with an undisturbed sediment-water interface were kept. Cores were packed carefully in foam-padded barrels with ice for transport to Michigan Technological University (MTU). One week elapsed between the time the first core was retrieved from New Croton Reservoir and the time that all cores were transferred to a controlled-environment room at MTU.

From one to four sediment cores from each station were extruded hydraulically and sliced into depth increments of one centimeter. The solid phase of the sediment sections were analyzed for water content (porosity), bulk density (total solids), loss-on-ignition (volatile solids), organic carbon content, total nitrogen content, total iron content, total manganese content, and total phosphorus content. The sediments were weighed, dried to constant weight at 65° C, and re-weighed for determination of bulk density and water content. A subsample of the sediments was ashed at 550° C overnight and reweighed for determination of loss-on-ignition.

Total carbon and total nitrogen were measured on sediment subsamples with a Carlo Erba Elemental Analyzer. Recovery of NIST standard Buffalo River Sediments was between 95 and 105% for both carbon and nitrogen. Comparison of carbon contents with loss-on-ignition values showed an excellent correlation ($r^2 = 0.97$, $n = 42$, $P < 0.01$) with 37% of the volatile solids being carbon. This relationship indicates that carbonate contents in the sediments were very low. In the results below, total carbon contents are reported and treated as organic carbon.

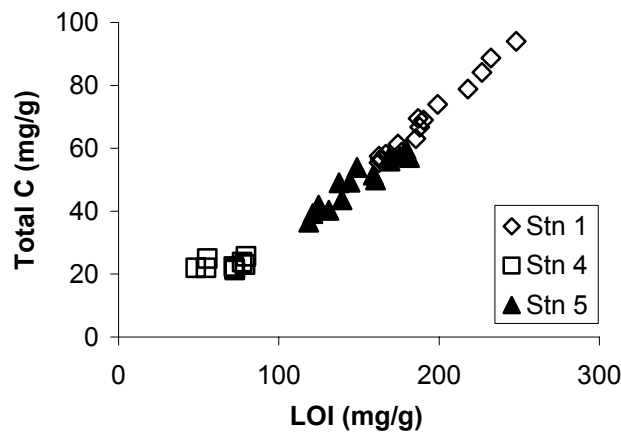


Figure 3-1 – New Croton reservoir: C content vs. Loss-on-Ignition (LOI)

Another aliquot of dried sediments was digested with HNO₃ in a microwave following EPA method 3051. The acid digestate was then analyzed by flame atomic absorption spectrophotometry for total iron and total manganese. The NIST standard Buffalo River Sediments subjected to the same digestion and analysis yielded a consistent recovery of 81 ± 7 % of the certified iron concentration. Because of the lower concentrations of manganese in the NIST standard, the recovery, 85 ± 25 %, was more variable. The concentrations reported below have not been corrected for the percentage recovery of either metal.

A third aliquot of wet sediment was digested with potassium permanganate to liberate phosphorus. The phosphorus then was measured by the ascorbic acid - molybdenum blue method (CLESCERI et al., 1998). Following digestion, the sediments were collected on a Nuclepore 0.4 μ m polycarbonate filter and dried to allow expression of the concentration on a dry-weight basis. The precision for total phosphorus measurements was ± 9 %.

Sediment stratigraphy results

A total of seven cores from the New Croton reservoir were extruded and analyzed for porosity, bulk density, and loss-on-ignition (i.e., volatile solids). One core from each of the three New Croton reservoir stations (NC-1, NC-4, NC-5) was analyzed for total carbon, total nitrogen and total phosphorus. Results of these analyses are presented in Figures 2 - 8 below.

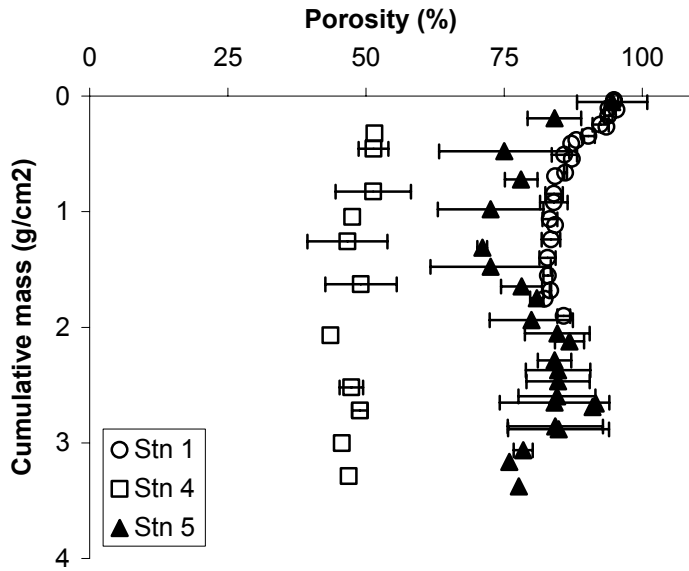


Figure 3-2 – New Croton Reservoir: Comparison of porosity at stations 1, 4, 5 (water content; error bars = ± 1 standard deviation)

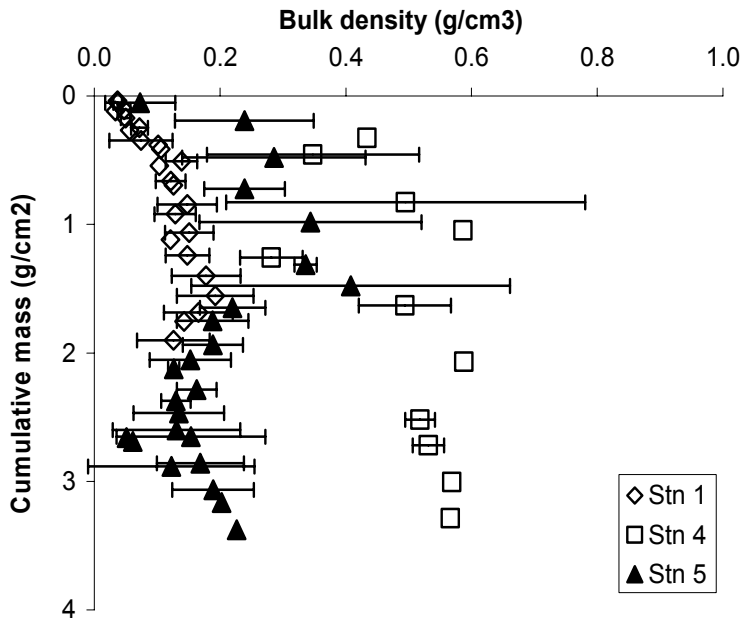


Figure 3-3 – New Croton Reservoir: Comparison of sediment bulk density at stations 1, 4, 5 (error bars = ± 1 standard deviation)

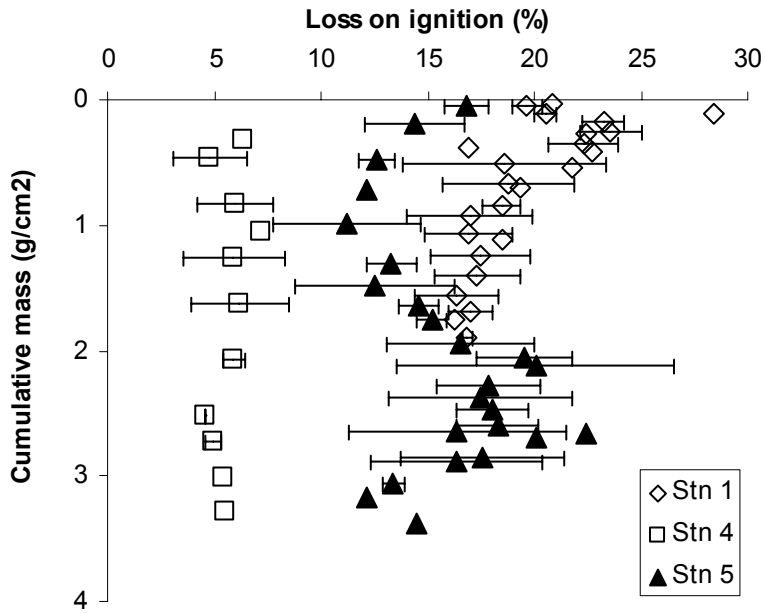


Figure 3-4 – New Croton Reservoir: Comparison of loss on ignition at stations 1, 4, 5 (error bars = ± 1 standard deviation)

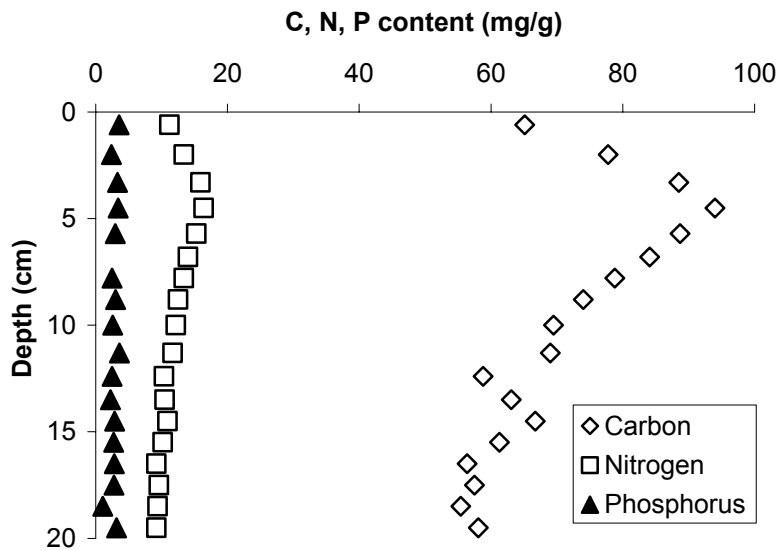


Figure 3-5 Profile of sediment carbon, nitrogen and phosphorus content for New Croton Reservoir Station 1.

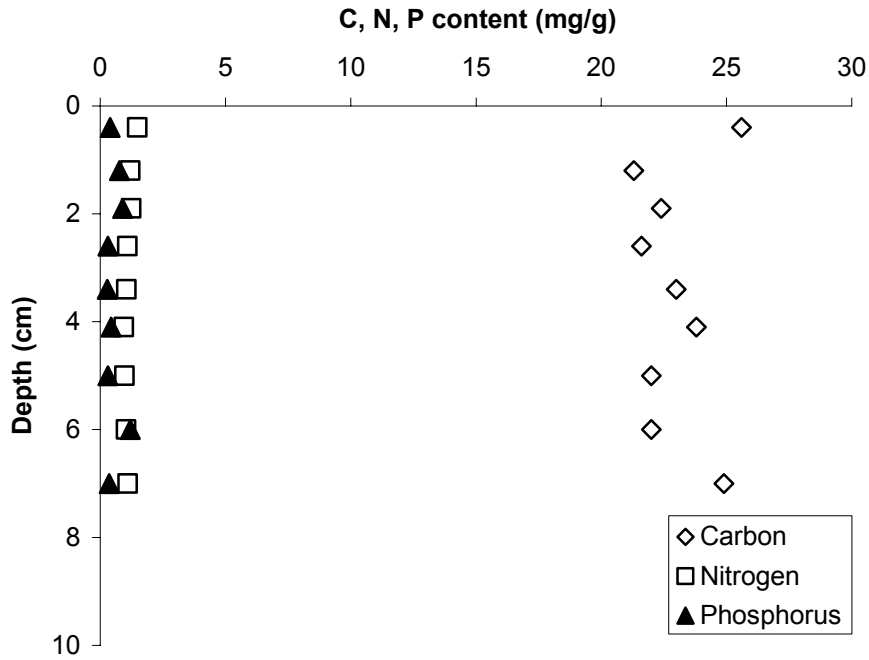


Figure 3-6 – New Croton Reservoir: Profiles of sediment C, N and P for Station 4

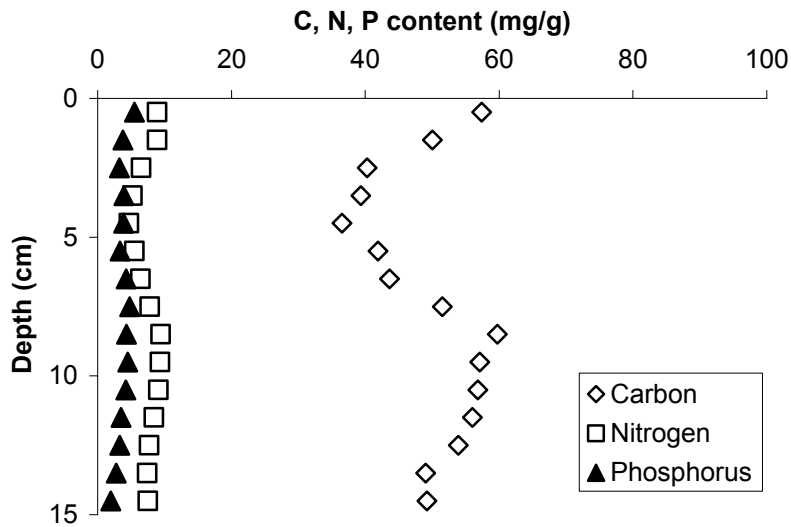


Figure 3-7 – New Croton Reservoir: Profiles of sediment C, N and P for Station 5

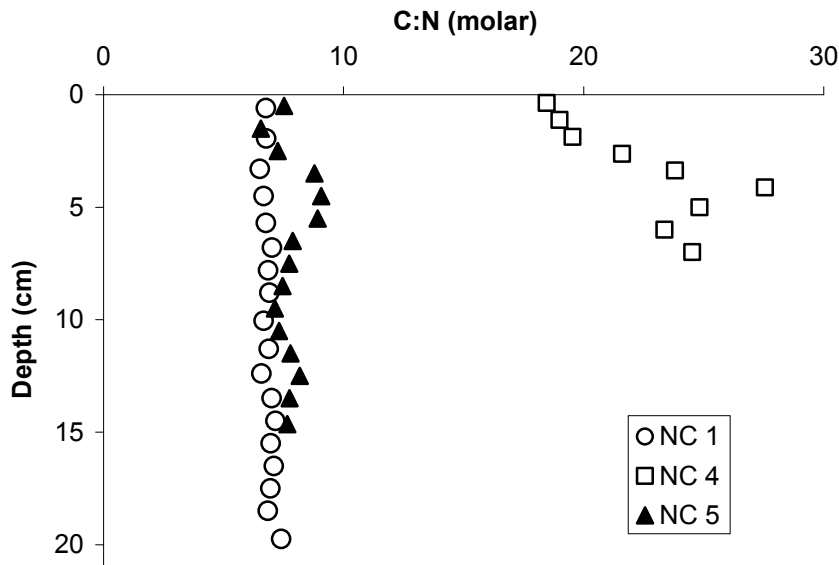


Figure 3-8 – New Croton Reservoir: Sediment profiles of C:N ratios at stations 1, 4, and 5

Total iron and total manganese were measured in the same cores that were analyzed for carbon, nitrogen and phosphorus. The coarse sediments at station 4 have lower Fe and Mn contents than do sediments at stations 1 and 5 both because concentrations are diluted by silica at station 4 and because the fine Fe and Mn oxides that are generated within the reservoir are focused to the same deep-water sites as is organic matter. The Mn profiles indicate that there is substantial release of Mn from the sediments into the water column. Because of the slow oxidation kinetics of Mn (e.g., FRIEDL et al., 1997), the Mn that is released from the sediments is reoxidized high in the water column. The flux of the fine particulate Mn oxides back to the sediments is proportional to the flux of organic matter (DAVIS and FORD, 1982) with greater amounts reaching station 1 than station 5. In contrast to Mn, there is little net movement of Fe from one station to another via the water column as indicated by the similar concentrations at stations 1 and 5. This lack of Fe mobility might result either from binding of the reduced iron with sulfide or from an adequate supply of oxygen in the hypolimnetic water (DAVISON and FINLAY, 1986).

Because of the faster oxidation kinetics of Fe, if oxygen is present in the water column the Fe is reoxidized either within the upper millimeters of sediments or in water immediately above the sediments. The sediments suggest that a considerable reduction in nutrient levels would be required to eliminate the flux of Mn into the hypolimnetic waters, and that control of Mn will be more difficult to achieve than control of Fe.

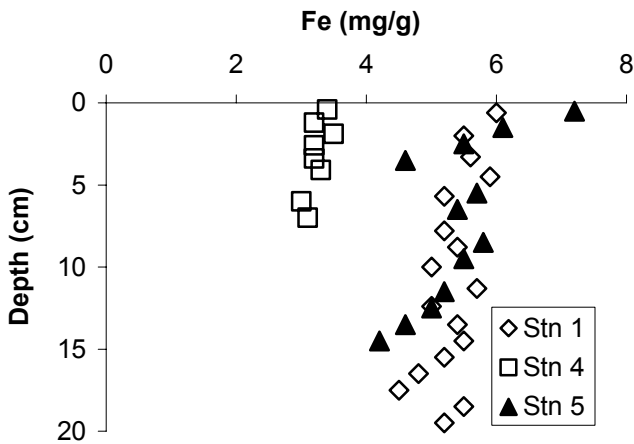


Figure 3-9 – New Croton Reservoir: Sediment profiles of total iron at stations 1, 4, 5

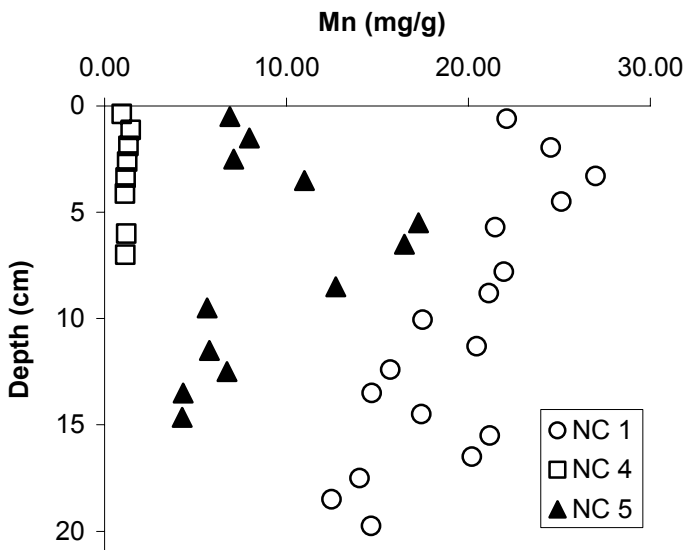


Figure 3-10 – New Croton Reservoir: Sediment profiles of Mn content at stations 1, 4 and 5

B) Sediment-water exchange rates

Methods and Materials

Sediment-water exchange rates were determined by measuring changes in solute concentrations in the water overlying sediment cores incubated under controlled conditions in the laboratory. The methods have been developed and refined over the past decade in this laboratory (e.g., ERICKSON and AUER, 1998; GELDA et al., 1995). Exchange rates were measured for oxygen (sediment oxygen demand, SOD), phosphorus, ammonia, iron, manganese, DOC and color.

The dissolved oxygen (DO) of the water overlying the sediment cores was measured by withdrawing water samples after intervals of 12 to 48 hours. The colorimetric technique of Parsons et al. (1984) was used to measure oxygen in the water samples. Sediment cores for SOD measurements were incubated at 8°C in the dark. After initial aeration of the overlying water to bring the DO concentration to 6-10 mg/L, the cores were capped with a two-holed rubber stopper. An inlet and outlet tube protruding from the cores functioned as a circulation system to mix the overlying water and to provide a means for withdrawing samples for periodic DO measurement. Water was continuously pumped from the outlet to the inlet tube, and water samples were withdrawn in triplicate every 18-24 hours over a 3-4 day period. Water that was withdrawn for DO measurements was replaced with hypolimnetic water from the appropriate reservoir; the oxygen demand of this water was measured separately and subtracted from the oxygen uptake of the cores. Empty core tubes filled with purified water were used as controls to account for oxygen leakage into the system.

As for SOD, sediment cores for ammonia and phosphorus measurements were incubated under controlled conditions of light (i.e., dark), temperature (8°C), and oxygen (oxic or anoxic), and water above the sediments was sampled periodically and analyzed for dissolved constituents. The pH and oxygen content of the water was maintained constant by aerating the water with a CO₂:N₂:O₂ gas mixture; the oxygen partial pressure was kept at either 0 (anoxic) or 20% (oxic). The volume of water removed for samples was replaced with filtered hypolimnetic water from the appropriate reservoirs; masses of solutes in the replacement water were subtracted from the mass accumulated in the water above the cores. Accumulation of dissolved solutes in the overlying water was used to calculate areal fluxes.

Results and Discussion

Oxygen concentrations decreased linearly above all sediment cores and changed negligibly in the control tubes. Rates of SOD were calculated as the slope of the regression line times the water volume divided by the area of the core. The variation among replicate cores from any one reservoir ranged from 10 to 50%; in all cases, the variability among cores was substantially larger than the uncertainty in the regression slope for an individual core.

Release rates of ammonia-nitrogen (NH₃-N) remained linear over at least one month. Rates of N release were measured for a total of 41 sediment cores; linear regressions (NH₃-N vs. time) were highly significant ($P < 0.05$) for all but two cores. Only the rates measured under anoxic conditions are reported here; rates measured under oxic conditions may underestimate the total release if nitrification occurred. As for SOD, variability among replicate cores (COV = 10-70%) was much larger than the uncertainty

in the release measured for single cores (COV < 10%). The total range in N release rates was 5.6-35 mg N/m²-d.

There was considerably more noise in the measured rates of phosphorus (P) exchange as compared to N release. Rates were measured under both oxic and anoxic conditions, and both positive (release) and negative (uptake) rates of exchange were observed under both oxic and anoxic conditions. Nevertheless, the average rate for all reservoirs measured under oxic conditions was negative (-0.11 mg P/m²-d) while the average rate measured under anoxic conditions was positive (+0.56 mg P/m²-d). As shown in Fig. 13, in individual reservoirs, P exchange rates generally were higher under anoxic as opposed to oxic conditions. In contrast to all other analytes, the uncertainty in P fluxes measured for a single core often was as large as the variability among replicate cores.

Rates of exchange of Fe²⁺, Mn²⁺, DOC and color were also measured for the three New Croton Reservoir stations. Under anoxic conditions, release rates of Fe²⁺ and Mn²⁺ were highly linear for nearly a month. As expected, release of iron was considerably reduced under oxic conditions. Because of the slower oxidation kinetics of Mn, exchange rates of Mn were more nearly comparable under oxic and anoxic conditions. As for Fe²⁺, release of color and DOC were substantially higher under anoxic as opposed to oxic conditions.

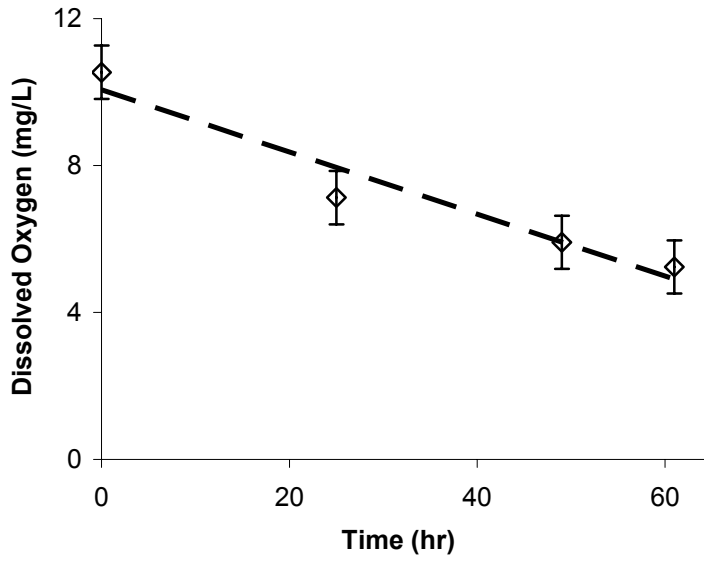


Figure 3-11 – New Croton Reservoir Station 1: Example of SOD measurements (error bars = ± 1 standard deviation)

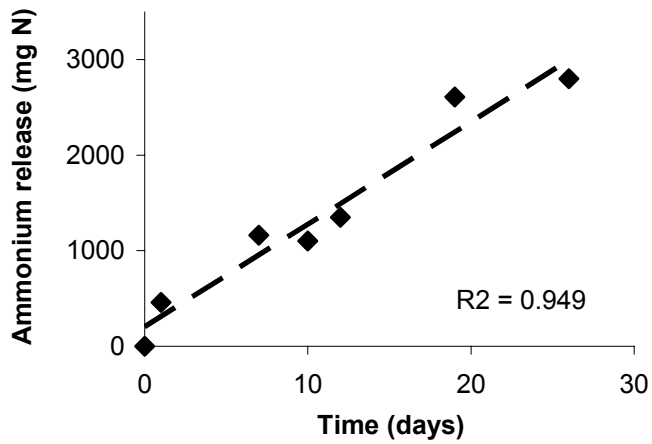


Figure 3-12 – New Croton Reservoir Station 5: Release of $\text{NH}_3\text{-N}$ from sediments

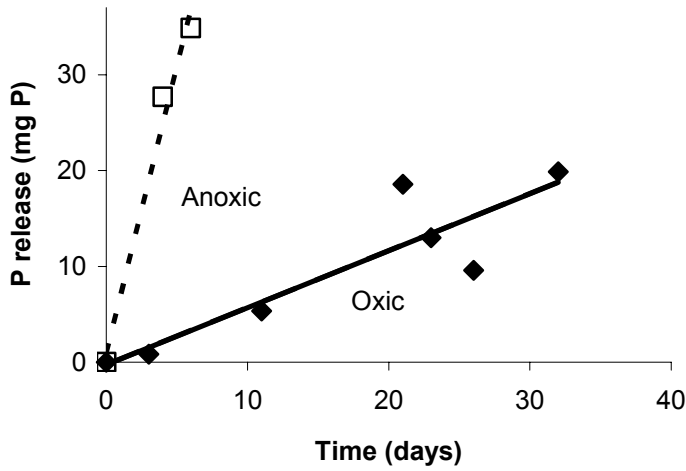


Figure 3-13 – New Croton Reservoir Station 1: P release from sediments under both oxic and anoxic conditions

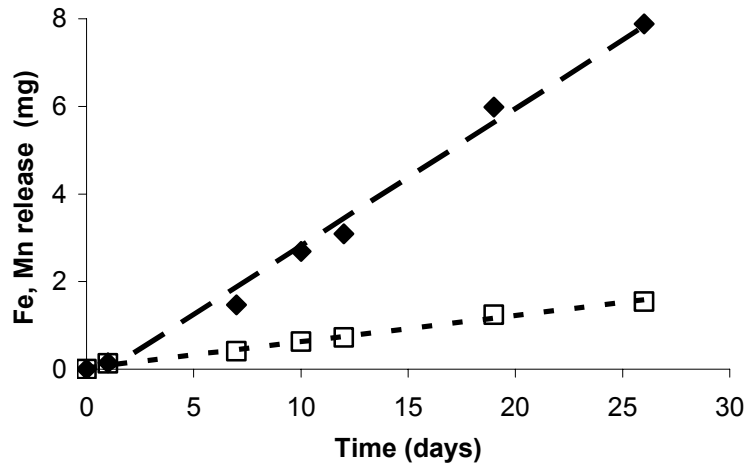


Figure 3-14 – New Croton Reservoir Station 5: Release of Fe²⁺ (solid diamonds) and Mn²⁺ (open squares) under anoxic conditions

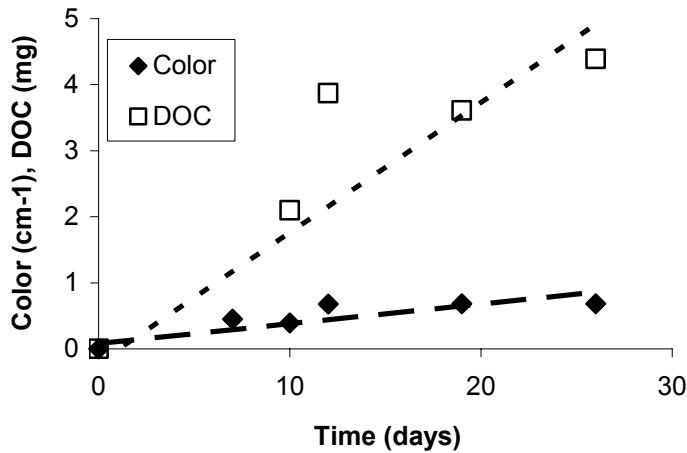


Figure 3-15 – New Croton Reservoir Station 5: Exchange of color and DOC above sediments

In many studies it has been found that the majority of the oxygen consumption in sediments is due to oxidation of reduced inorganic species rather than to direct oxidation of organic matter (CANFIELD et al., 1993; SWEERTS et al., 1991). In coastal marine sediments, as little as 10% of the oxygen may be consumed directly by heterotrophic bacteria. In contrast, the oxidation of reduced species measured in this study (Fe^{2+} , Mn^{2+} , NH_3) could contribute only 13%, on average, to the measured SOD even if the entire quantity of these substances released under anaerobic conditions were to be oxidized. The disparity between this study and previous studies suggests that other reduced substances (e.g., H_2S , CH_4) that were not measured in this study may account for a large portion of the oxygen uptake. If in the future it becomes desirable to model oxygen consumption in more detail, some measurement of these reduced species might be warranted.

Appendix 2: Model Framework

Box-Models

In recent decades many different modeling frameworks for early diagenesis have been developed. They vary in the spatial representation of the system as well as the level of complexity with which biological, chemical, and physical processes are modeled. The most common approach is based on one-dimensional partial differential equations including various diagenetic processes such as chemical reactions, diffusion, advection, adsorption, burial, and compaction (BERNER, 1980; BOUDREAU, 1996). Concentration profiles of both solid species (e.g., organic matter, FeS, Fe(OH)₃, MnO) and dissolved species (e.g., O₂, NO₃⁻, SO₄²⁻, NH₄⁺, CH₄) are computed (e.g., BILLEN, 1982; HUNTER et al., 1998; KELLY-GERREYN et al., 1999; KLUMP and MARTENS, 1989; PARK and JAFFÉ, 1999; SOETAERT et al., 1996; VAN CAPPELLEN and YIFENG, 1996). Nutrient fluxes into the overlying water can then be calculated from concentration gradients at the sediment surface using Fick's first law. The effects of bioturbation and bioirrigation on the transport of solid and dissolved species may also be included (e.g., BOUDREAU and MARINELLI, 1994; VAN CAPPELLEN and YIFENG, 1996).

Another type of model proposed by Di Toro (2001), represents the sediment as two layers: a thin, surface layer, and the underlying bulk sediment. The mathematical representation is based on mass balance equations, and nutrient fluxes can be computed using mass transfer coefficients. This formulation can easily be integrated into comprehensive water quality models and simplifies investigation of different kinetic formulations for the prediction of sediment nutrient release.

Diagenetic processes are driven by inputs of organic matter from the water column. The magnitude of the sedimentation flux, J (g solids $\text{cm}^{-2} \text{day}^{-1}$), and the average organic carbon content, o (gC g solids $^{-1}$), of the settling solids are functions of catchment size, lake morphometry, trophic status, and hydraulic regime of the lake (GORHAM et al., 1983; GORHAM et al., 1974; TARTARI and BIASCI, 1997). The two sediment layers are defined by their thickness, H (cm), and their solids concentration, m (g solids cm^{-3}), the latter depending on particle properties (e.g., particle size distribution and density) and deposition processes (DI TORO, 2001). The organic matter is decomposed microbially, and any residual is buried in the underlying sediment. This output flux is modeled using a burial velocity, w (cm day^{-1}). In the lower layer (Box 2), the direct input of settling particles is replaced by the burial flux of partly decomposed material from the surface layer (Box 1).

Surface layer (Box 1):

$$\frac{dC_1}{dt} = -rxn - \frac{w \cdot C_1}{H_1} + \frac{o \cdot J}{H_1} \quad (1)$$

Bottom layer (Box 2):

$$\frac{dC_2}{dt} = -rxn - \frac{w \cdot C_2}{H_2} + \frac{w \cdot C_1}{H_2} \quad (2)$$

Variables C_1 and C_2 (g cm^{-3}) represent concentrations of substrate pools, e.g., organic carbon or organic nitrogen.

For dissolved species, diffusion terms are included into the mass balance. Mass transfer coefficients, T_D (day^{-1}), that are related to molecular diffusion coefficients or bioturbation rates can be used to model this process (BIRD et al., 1960; in DI TORO, 2001).

Surface layer (Box 1):

$$\frac{dD_1}{dt} = +rxn - T_D \cdot (D_1 - D_0) + T_D \cdot (D_2 - D_1) \quad (3)$$

Bottom layer (Box 2):

$$\frac{dD_2}{dt} = +rxn - T_D \cdot (D_2 - D_1) \quad (4)$$

Variables D_0 , D_1 , and D_2 (g cm^{-3}) are concentrations of dissolved species in the overlying water, the surface layer, and the bottom layer, respectively.

Decomposition kinetics

Decomposition of organic matter in sediments is complex and not fully understood. The complex mixture of biochemical substrates is sequentially broken down by mutualistic consortia of bacteria eventually leading to the formation of inorganic nutrients (FENCHEL et al., 1998). Decomposition models are therefore always based on simplifying assumptions. The objective of this study is to compare the commonly used multi-G model (WESTRICH and BERNER, 1984) with a more mechanistic approach.

Westrich and Berner (1984) have shown that the decomposition process follows first-order kinetics and that the organic matter can be divided into a labile fraction, C_l , and a stable fraction, C_s , with significantly different reactivities, k_l and k_s , and a refractory fraction, C_r , that is not decomposed at all on a time scale relevant to water quality modeling.

$$rxn_l = k_l \cdot C_l \quad (5)$$

$$rxn_s = k_s \cdot C_s \quad (6)$$

$$rxn_r = 0 \quad (7)$$

To better represent the effect of substrate quality, several refinements have been made to the multi-G model (e.g., BOSATTA and ÅGREN, 1991; BOUDREAU and RUDDICK, 1991; MIDDELBURG, 1989), but none of the formulations for organic matter decomposition in sediments explicitly includes the effect of microbial biomass. Most mineralization reactions, however, are either directly performed by bacteria or biologically mediated (CAPONE and KIENE, 1988). Studies of decomposition of soil organic matter on the other hand have led to the development of more mechanistic models including biomass pools and the corresponding processes such as nutrient mineralization, immobilization, and growth limitation (e.g., ABRAHAMSEN and HANSEN, 2000; BLAGODATSKY and RICHTER, 1998; MCGILL et al., 1981; PARNAS, 1975; PAUL and JUMA, 1981; VAN VEEN et al., 1981).

The model presented in this study (BIOSED) combines the two approaches and is based on five main assumptions:

- 1) Breakdown of organic matter is proportional to the concentration of decomposers, C_b (gC cm⁻³), in the system;
- 2) Organic matter is subdivided into labile, stable, and refractory substrate pools according to the multi-G model;
- 3) A constant microbial efficiency, *eff*, determines the fraction of substrate carbon respired;
- 4) Carbon and nitrogen cycles are coupled using fixed but distinct C:N ratios for all substrate pools and the biomass pool;
- 5) The size of the biomass pool is limited by a constant “recycling rate” that integrates such factors as competition, death, and predation.

Mathematically, the dependence of the decomposition kinetics on microbial biomass is included by introducing a dimensionless biomass concentration C_b/C_{b0} (i.e., proportionality factor). A dimensionless factor simplifies the comparison of the two models, since identical rate constants can be used in both frameworks. The change in microbial biomass follows

$$\frac{dC_b}{dt} = \frac{C_b}{C_{b0}} \cdot (k_l \cdot C_l + k_s \cdot C_s) - r \cdot C_b \quad (4)$$

where C_b is the biomass carbon concentration, C_{b0} is the biomass normalization factor, and r is a constant microbial death rate. Bacteria require carbon substrate for their assimilatory and dissimilatory metabolism and therefore have to decompose more substrate than the amount taken up for cell growth. In microbial ecology this is commonly expressed as a constant growth yield or C uptake efficiency. Thus, substrate breakdown follows

Labile substrate pool C_l :

$$rxn_l = \frac{1}{eff} \cdot \frac{C_b}{C_{b0}} k_l \cdot C_l \quad (8)$$

Stable substrate pool C_s :

$$rxn_s = \frac{1}{eff} \cdot \frac{C_b}{C_{b0}} k_s \cdot C_s \quad (9)$$

Refractory substrate pool C_r :

$$rxn_r = 0 \quad (10)$$

Whether bacteria are limited by the availability of substrate carbon or substrate nitrogen depends on the overall C:N ratio of the decomposable organic matter, the microbial C:N ratio, and microbial C assimilation efficiency (PARNAS, 1975). This

conceptualization assumes that the efficiency for N uptake is 100 percent. According to recent studies, however, bacteria are not able to take up nitrogen without any losses (LEHMANN et al., 2002). Applying the Parnas simplification, carbon limitation occurs when

$$CN_{sub} < \frac{CN_b}{eff} \quad (11)$$

where CN_{sub} and CN_b are substrate and biomass C:N ratios, respectively. Microbial growth is nitrogen limited when

$$CN_{sub} > \frac{CN_b}{eff} \quad (12)$$

In the literature on lake sediment processes, no evidence for nitrogen limited growth of bacteria was found. A rough estimation based on typical values for microbial C:N ratios and efficiencies also suggests that nitrogen-limitation will not occur in most lacustrine systems if bacterial C efficiencies are <25%. Therefore nitrogen pool sizes and breakdown are determined by the corresponding carbon pools and rates:

$$\frac{dNitrogen}{dt} = \frac{1}{C:N} \cdot \frac{dCarbon}{dt} \quad (13)$$

Since the rate of breakdown of organic matter in both the multi-G model and the BIOSSED model is proportional to the substrate pool sizes (first-order kinetics), the microbial growth rate is not limited. The classic model for single substrate-limited bacterial growth was proposed by Monod (1942). Multiple variations of the same concept have been developed and extended to include multiple food sources (see KOVAROVA-KOVAR and EGLI, 1998 for an excellent review). These empirical models are mainly based on bacteria batch cultures growing under controlled conditions and feeding on

known types and concentrations of substrate. Many decomposition models in soils literature are based on this approach (e.g., BLAGODATSKY and RICHTER, 1998; PARNAS, 1975; VAN VEEN et al., 1981), whereas most sediment diagenesis models are based on simpler, first-order kinetics.

From a mechanistic point of view it might be desirable to replace the first-order kinetics with double-substrate Monod kinetics in a decomposition model. This modification, however, results in a number of parameters for which no values are available. Whereas halfsaturation constants for defined growth media can be determined experimentally, halfsaturation constants for labile and stable organic matter can only be calculated as fitting parameters. Moreover, breakdown of organic matter is a complex process involving several distinct steps and different microbial populations. Organic polymers are hydrolyzed by extracellular enzymes and their constituents are then taken into bacterial cells and further processed (FENCHEL et al., 1998). Both first-order kinetics and Monod kinetics lump these processes into one rate expression. The most accurate prediction will result from a formulation that captures the kinetics of the rate limiting step. First-order kinetics reduces the number of fitting parameters, and evidence that hydrolysis is the rate-limiting step (KRISTENSEN and HANSEN, 1995 and references therein) supports our choice as a valid simplification.

Reference Scenario

The objective of this modeling study is to compare two different kinetic representations of organic matter decomposition and to elucidate general principles that apply to a wide range of sediments. Therefore, a reference scenario was chosen, in which steady-state rates of organic matter breakdown in the surface layer of both models are set

to be equal. Deviations from the reference scenario are then used to determine the effects of various parameters and environmental variables on the multi-G and the BIOSED model.

Model sediment properties (porosity, solids concentration) were chosen to mimic Dollar Bay sediments (see Experimental Methods section for details). No measured sedimentation rates are available for the study area; therefore a burial velocity, w , of 0.72 cm/yr was estimated. Being in the upper range of values reported (0.1 – 1.0 cm/yr, DI TORO, 2001) this velocity corresponds to a mesotrophic to eutrophic system. Organic matter content of settling particles can be estimated from desired initial organic matter content in the surface sediment and kinetic parameters using the analytical solution of the steady-state system. Organic matter input is the driving force behind all diagenetic processes. Its effect on carbon and nitrogen mineralization is examined in this study. In the reference scenario 30% of all settling material is assumed to be organic matter.

Fractions and properties of labile, stable, and refractory substrate were not determined in this study, and literature values for this conceptual fractionation are inconsistent and depend on various environmental parameters. Decomposition experiments with different electron acceptors (O_2 , SO_4^{2-} , NO_3^- , HARVEY et al., 1995; KRISTENSEN and HANSEN, 1995; KRISTENSEN and HOLMER, 2001; LEHMANN et al., 2002) as well as experiments with different substrate qualities (e.g., fresh and aged diatoms vs. fresh and aged barley hay, KRISTENSEN and HOLMER, 2001) revealed some of the environmental controls on decomposition kinetics. For both the multi-G and the BIOSED model, reference values of relative abundances in the sedimentation flux were taken from Westrich and Berner (1984) and rounded to the next multiple of five. First-order decay

constants, k_l and k_s , were taken from the same publication. Labile substrate is a conglomerate of easily decomposable organic macromolecules such as simple sugars and amino acids (BURDIGE, 1991; HEDGES et al., 2001). For the sake of model simplicity, the C:N ratio of the labile substrate was assumed to equal the ratio in bacterial biomass (molar C:N = 6.5). Terrestrial input contributes more stable material such as lignin or cellulose. Stable organic matter was therefore attributed a C:N ratio typical of terrestrial material (13-600, URBAN et al., 2002). Refractory organic matter is even harder to characterize. Assuming that after sufficient time all labile and stable organic matter is completely mineralized, organic C:N ratios of deep sediments correspond to the refractory C:N ratio. Most lake sediments show depth profiles with steady-state C:N ratios between 11 and 15 (URBAN et al., 2002). Since neither the fractions nor the properties of the different pools can directly be based on experimental data, model sensitivity to changes in these parameters is evaluated.

The steady-state biomass concentration in the sediment surface layer was assumed to be a constant fraction of total organic carbon. The model value of ~12% is in the range of experimental results reported in the literature (GÄCHTER et al., 1988; TÖRNBLOM and BOSTRÖM, 1995). Microbial C uptake efficiencies in sediments are poorly known but are believed to be low (cf., GOLDMAN and DENNETT, 2000; HARVEY et al., 1995). In the BIOSSED model only 10% of substrate C is taken up for biomass growth, the remainder is respired. Given the assumption of equal decomposition rates in the surface box (Box 1) of the multi-G and the BIOSSED model, the analytical solution can be solved for the biomass normalization constant, C_{b0} , and the recycling rate, r . Biomass doubling time in

the surface layer equals ~ 100 days. Literature values, e.g., for a temperate eutrophic lake, are in the same range (TÖRNBLOM and BOSTRÖM, 1995).

Layer thickness, H_l , and burial velocity, w , are related to the residence time, τ , of sediment particles in the box. A layer thickness for the surface box of 0.3 cm corresponds to a typical value used for sediment core stratigraphy. It translates into a residence time of 150 days, which equals ~ 1.5 biomass doubling times in the BIOSSED model.

Mathematical representation

Table 3-1 – Differential equations: two-box multi-G model

labile substrate $C_{l,1}$ (Box 1)	$\frac{dC_{l,1}}{dt} = -k_l \cdot C_{l,1} - \frac{w \cdot C_{l,1}}{H_1} + \frac{f_l \cdot J_c}{H_1}$
labile substrate $C_{l,2}$ (Box 2)	$\frac{dC_{l,2}}{dt} = -k_l \cdot C_{l,2} - \frac{w \cdot C_{l,2}}{H_2} + \frac{w \cdot C_{l,1}}{H_2}$
stable substrate $C_{s,1}$ (Box 1)	$\frac{dC_{s,1}}{dt} = -k_s \cdot C_{s,1} - \frac{w \cdot C_{s,1}}{H_1} + \frac{f_s \cdot J_c}{H_1}$
stable substrate $C_{s,2}$ (Box 2)	$\frac{dC_{s,2}}{dt} = -k_s \cdot C_{s,2} - \frac{w \cdot C_{s,2}}{H_2} + \frac{w \cdot C_{s,1}}{H_2}$
refractory substrate $C_{r,1}$ (Box 1)	$\frac{dC_{r,1}}{dt} = -\frac{w \cdot C_{r,1}}{H_1} + \frac{f_r \cdot J_c}{H_1}$
refractory substrate $C_{r,2}$ (Box 2)	$\frac{dC_{r,2}}{dt} = -\frac{w \cdot C_{r,2}}{H_2} + \frac{w \cdot C_{r,1}}{H_2}$
substrate $N_{i,j}$ ($i = l, s, r; j = 1, 2$)	$\frac{dN_{i,1}}{dt} = \frac{1}{CN_i} \cdot \frac{dC_{i,1}}{dt}$
$CO_{2,1}$ (Box 1)	$\begin{aligned} \frac{dCO_{2,1}}{dt} &= k_l \cdot C_{l,1} + k_s \cdot C_{s,1} \\ &- T_{C,0-1} \cdot (CO_{2,1} - CO_{2,0}) + T_{C,1-2} \cdot (CO_{2,2} - CO_{2,1}) \end{aligned}$
$CO_{2,2}$ (Box 2)	$\frac{dCO_{2,2}}{dt} = k_l \cdot C_{l,2} + k_s \cdot C_{s,2} - T_{C,1-2} \cdot (CO_{2,2} - CO_{2,1})$

NH_{3,1} (Box 1)	$\frac{dNH_{3,1}}{dt} = \frac{1}{CN_l} \cdot k_l \cdot C_{l,1} + \frac{1}{CN_s} \cdot k_s \cdot C_{s,1} - T_{N,0-1} \cdot (NH_{3,1} - NH_{3,0}) + T_{N,1-2} \cdot (NH_{3,2} - NH_{3,1})$
NH_{3,2} (Box 2)	$\frac{dNH_{3,2}}{dt} = \frac{1}{CN_l} \cdot k_l \cdot C_{l,2} + \frac{1}{CN_s} \cdot k_s \cdot C_{s,2} - T_{N,1-2} \cdot (NH_{3,2} - NH_{3,1})$

Table 3-2 – Differential Equations: two-box BIOSED model

labile sub. C_{l,1} (Box 1)	$\frac{dC_{l,1}}{dt} = -\frac{C_{b,1}}{eff \cdot C_{b0}} \cdot k_l \cdot C_{l,1} - \frac{w \cdot C_{l,1}}{H_1} + \frac{f_l \cdot J_c}{H_1} + r \cdot C_{b,1}$
labile sub. C_{l,2} (Box 2)	$\frac{dC_{l,2}}{dt} = -\frac{C_{b,2}}{eff \cdot C_{b0}} \cdot k_l \cdot C_{l,2} - \frac{w \cdot C_{l,2}}{H_2} + \frac{w \cdot C_{l,1}}{H_2} + r \cdot C_{b,2}$
stable sub. C_{s,1} (Box 1)	$\frac{dC_{s,1}}{dt} = -\frac{C_{b,1}}{eff \cdot C_{b0}} \cdot k_s \cdot C_{s,1} - \frac{w \cdot C_{s,1}}{H_1} + \frac{f_s \cdot J_c}{H_1}$
stable sub. C_{s,2} (Box 2)	$\frac{dC_{s,2}}{dt} = -\frac{C_{b,2}}{eff \cdot C_{b0}} \cdot k_s \cdot C_{s,2} - \frac{w \cdot C_{s,2}}{H_2} + \frac{w \cdot C_{s,1}}{H_2}$
refract. sub. C_{r,1} (Box 1)	$\frac{dC_{r,1}}{dt} = -\frac{w \cdot C_{r,1}}{H_1} + \frac{f_r \cdot J_c}{H_1}$
refract. sub. C_{r,2} (Box 2)	$\frac{dC_{r,2}}{dt} = -\frac{w \cdot C_{r,2}}{H_2} + \frac{w \cdot C_{r,1}}{H_2}$
biomass C_{b,1} (Box 1)	$\frac{dC_{b,1}}{dt} = \frac{C_{b,1}}{C_{b0}} \cdot (k_l \cdot C_{l,1} + k_s \cdot C_{s,1}) - \frac{w \cdot C_{b,1}}{H_1} - r \cdot C_{b,1}$
biomass C_{b,2} (Box 2)	$\frac{dC_{b,2}}{dt} = \frac{C_{b,2}}{C_{b0}} \cdot (k_l \cdot C_{l,2} + k_s \cdot C_{s,2}) - \frac{w \cdot C_{b,2}}{H_2} + \frac{w \cdot C_{b,1}}{H_2} - r \cdot C_{b,2}$

$N_{i,j}$ ($i = l, s, r, b;$ $j = 1, 2$)	$\frac{dN_{i,j}}{dt} = \frac{1}{CN_i} \cdot \frac{dC_{i,j}}{dt}$
$CO_{2,1}$ (Box 1)	$\frac{dCO_{2,1}}{dt} = \frac{(1-eff) \cdot C_{b,1}}{eff \cdot C_{b0}} \cdot (k_l \cdot C_{l,1} + k_s \cdot C_{s,1})$ $- T_{C,0-1} \cdot (CO_{2,1} - CO_{2,0}) + T_{C,1-2} \cdot (CO_{2,2} - CO_{2,1})$
$CO_{2,2}$ (Box 2)	$\frac{dCO_{2,2}}{dt} = \frac{(1-eff) \cdot C_{b,2}}{eff \cdot C_{b0}} \cdot (k_l \cdot C_{l,2} + k_s \cdot C_{s,2})$ $- T_{C,1-2} \cdot (CO_{2,2} - CO_{2,1})$
$NH_{3,1}$ (Box 1)	$\frac{dNH_{3,1}}{dt} = \frac{C_{b,1}}{C_{b0}} \cdot \left[k_l \cdot C_{l,1} \cdot \left(\frac{1}{eff \cdot CN_l} - \frac{1}{CN_b} \right) + k_s \cdot C_{s,1} \cdot \left(\frac{1}{eff \cdot CN_s} - \frac{1}{CN_b} \right) \right]$ $- T_{N,0-1} \cdot (NH_{3,1} - NH_{3,0}) + T_{N,1-2} \cdot (NH_{3,2} - NH_{3,1})$
$NH_{3,2}$ (Box 2)	$\frac{dNH_{3,2}}{dt} = \frac{C_{b,2}}{C_{b0}} \cdot \left[k_l \cdot C_{l,2} \cdot \left(\frac{1}{eff \cdot CN_l} - \frac{1}{CN_b} \right) + k_s \cdot C_{s,2} \cdot \left(\frac{1}{eff \cdot CN_s} - \frac{1}{CN_b} \right) \right]$ $- T_{N,1-2} \cdot (NH_{3,2} - NH_{3,1})$

Table 3-3 – Analytical solution: two-box multi-G model

labile substrate $C_{l,1,ss}$ (Box 1)	$C_{l,1,ss} = \frac{f_l \cdot J_c}{k_l \cdot H_1 + w}$
labile substrate $C_{l,2,ss}$ (Box 2)	$C_{l,2,ss} = \frac{w \cdot C_{l,1,ss}}{k_l \cdot H_2 + w}$
stable substrate $C_{s,1,ss}$ (Box 1)	$C_{s,1,ss} = \frac{f_s \cdot J_c}{k_s \cdot H_1 + w}$
stable substrate $C_{s,2,ss}$ (Box 2)	$C_{s,2,ss} = \frac{w \cdot C_{s,1,ss}}{k_s \cdot H_2 + w}$

refractory substrate $C_{r,1,ss}$ (Box 1)	$C_{r,1,ss} = \frac{f_r \cdot J_c}{w}$
refractory substrate $C_{r,2,ss}$ (Box 2)	$C_{r,2,ss} = C_{r,1,ss}$

Table 3-4 – Analytical solution: two-box BIOSED model

labile substrate $C_{l,1,ss}$ (Box 1)	$C_{l,1,ss} = \frac{eff \cdot C_{b0} \cdot (f_l \cdot J_c + r \cdot H_1 \cdot C_{b,1,ss})}{k_l \cdot H_1 \cdot C_{b,1,ss} + eff \cdot C_{b0} \cdot w}$
labile substrate $C_{l,2,ss}$ (Box 2)	$C_{l,2,ss} = \frac{eff \cdot C_{b0} \cdot (w \cdot C_{l,1,ss} + r \cdot H_2 \cdot C_{b,2,ss})}{k_l \cdot H_2 \cdot C_{b,2,ss} + eff \cdot C_{b0} \cdot w}$
stable substrate $C_{s,1,ss}$ (Box 1)	$C_{s,1,ss} = \frac{eff \cdot C_{b0} \cdot f_s \cdot J_c}{k_s \cdot H_1 \cdot C_{b,1,ss} + eff \cdot C_{b0} \cdot w}$
stable substrate $C_{s,2,ss}$ (Box 2)	$C_{s,2,ss} = \frac{eff \cdot C_{b0} \cdot w \cdot C_{s,1,ss}}{k_s \cdot H_2 \cdot C_{b,2,ss} + eff \cdot C_{b0} \cdot w}$
refract. substrate $C_{r,1,ss}$ (Box 1)	$C_{r,1,ss} = \frac{f_r \cdot J_c}{w}$
refract. substrate $C_{r,2,ss}$ (Box 2)	$C_{r,2,ss} = C_{r,1,ss}$

biomass $C_{b,1,ss}$ (Box 1)	$C_{b,1,ss} = \frac{eff \cdot C_{b0} \cdot (w \cdot C_{l,1,ss} - f_l \cdot J_c)}{k_l \cdot H_1 \cdot C_{l,1,ss} \cdot (eff - 1) + eff \cdot H_1 \cdot k_s \cdot C_{s,1,ss} - eff \cdot C_{b0} \cdot w}$
biomass $C_{b,2,ss}$ (Box 2)	$C_{b,2,ss} = \frac{eff \cdot C_{b0} \cdot w \cdot (C_{l,2,ss} - C_{l,1,ss} - C_{b,1,ss})}{k_l \cdot H_2 \cdot C_{l,2,ss} \cdot (eff - 1) + eff \cdot H_2 \cdot k_s \cdot C_{s,2,ss} - eff \cdot C_{b0} \cdot w}$

Table 3-5 – Common model parameters (multi-G, BIOSED)

Constants/Parameters		Model value	
solids concentration	$m =$	0.2	(g/cm ³)
labile C:N ratio	$CN_l =$	6.5	(gC/gN)
stable C:N ratio	$CN_s =$	26	(gC/gN)
refractory C:N ratio	$CN_r =$	15	(gC/gN)
rate constant labile pool	$k_l =$	24	(1/yr)
rate constant stable pool	$k_s =$	1.4	(1/yr)
mass transfer coefficient CO ₂ (Box 1 – water)	$T_{C,0-1} =$	2.55	(1/d)
mass transfer coefficient NH ₃ (Box 1 – water)	$T_{N,0-1} =$	3.03	(1/d)
mass transfer coefficient CO ₂ (Box 2 – Box 1)	$T_{C,1-2} =$	0.53	(1/d)
mass transfer coefficient NH ₃ (Box 2 – Box 1)	$T_{N,1-2} =$	0.63	(1/d)

Table 3-6 – Specific model parameters (BIOSED model)

Constants/Parameters		Model value
microbial efficiency	eff =	0.1 (-)
biomass recycling	r =	0.33 (1/yr)
biomass normalizing factor	C _{b0} =	0.016 (g C /cm ³)

Table 3-7 – Reference scenario

Constants/Parameters		Model value
burial velocity	w =	0.72 (cm/yr)
sedimentation flux	J =	0.14 (g /cm ² yr)
OM in sedimentation flux	o _j =	30 (%)
labile fraction in sedimentation flux	f _l =	60 (%)
stable fraction in sedimentation flux	f _s =	15 (%)
refractory fraction in sedimentation flux	f _r =	25 (%)
residence time in Box 1	τ ₁ =	150 (d)
thickness of Box 1	H ₁ =	0.3 (cm)
residence time in Box 2	τ ₂ =	3000 (d)
thickness of Box 2	H ₂ =	6.00 (cm)

Table 3-8 - One-box steady-state pools and fluxes (reference scenario)

Box 1 pools/fluxes		multi-G model		BIOSED model	
labile substrate C pool	$C_{l1} =$	1.64E-3	(g /cm ³)	1.66E-3	(g /cm ³)
stable substrate C pool	$C_{s1} =$	2.84E-3	(g /cm ³)	2.84E-3	(g /cm ³)
refractory substrate C pool	$C_{r1} =$	7.50E-3	(g /cm ³)	7.50E-3	(g /cm ³)
CO ₂ flux (Box 1 – water)	$J_{CO_2,01} =$	1.2E-4	(g /cm ² yr)	1.1E-4	(g /cm ² yr)
NH ₃ flux (Box 1 – water)	$J_{NH_3,01} =$	2.0E-5	(g /cm ² yr)	1.8E-5	(g /cm ² yr)
biomass C pool	$C_{b,1} =$	-	-	1.60E-3	(g /cm ³)

Appendix 3: Experimental Protocols

Sediment amendments, Sample preparation

Material and Reagents

- 1000 mL wash bottle and tubing
- 50-mL glass incubation bottles w/ cap and septum
- Various beakers
- 1.5 L glass jars with lids
- Mechanic paddle stirrer
- 25-mL plastic pipette

- Sodium Nitrate (solid)
- Glycine solution (100g/L)
- Algae (*Selenastrum c.*)
- Sieved sediment

~ three days before start of incubation

- Deoxygenate milli-Q needed to prepare sediment slurry (bubble with N₂ for ~2 hrs)
- Dilute sediment with milli-Q according to centrifugation experiments
- Add Sodium Nitrate according to organic matter content
- Mix mechanically at low speed for ~2 hrs
- Store in sealed glass jars at 4°C

start of incubation

- for substrate addition experiments: add appropriate amount of Glycine or Algae to sediment slurry (Dollar Bay sediments only)
- Use 25-mL pipette to fill 50-mL vials
No headspace; air bubbles should be removed by piercing septum!
- Incubate in tumbler at 20°C

Take and process incubation samples

Material and Reagents

- Flow-thru cell, pH electrode, and pH-meter
- 10-100 μL pipette tips
- Syringe needles
- 30-mL syringes
- 2-mL syringe
- 5-mL glass vials for biomass samples
- 30-mL plastic vials for NH_3 samples
- 100-1000 μL pipette
- 50-mL glass beakers
- Centrifuge
- Balance

- Milli-Q
- Nitrogen gas
- EDTA solution (75 g/L)

pH measurements and Fe complexation

- Take samples from tumbler (1 - 3 per treatment)
- Shake incubation vial manually
- Pierce septum with pipette tip and connect to flow-thru cell
- Attach pH probe to flow-thru cell
- Pierce septum and use 30-mL syringe to inject $\sim 5\text{mL}$ of N_2 ; slurry is displaced into cell
- Measure pH
- Remove cell and pipette tip
- Inject 1 mL of EDTA solution into incubation vial (2-mL syringe)
- Mix well by shaking manually
Rinse cell and probe thoroughly between samples!

Centrifugation; NH₃ and alkalinity samples

- Balance centrifuge
- Centrifuge incubation vials at ~1900 rpm for 25 minutes
Do not exceed this speed!
- Withdraw 0.5 - 1 mL of supernatant for NH₃ analysis;
Store samples in 30-mL plastic bottles at -23°C
- Carefully pour supernatant into 50-mL beakers
Avoid resuspension!
- Weigh supernatant (sample volume for alkalinity titration)
- Supernatant should be analyzed for ΣCO₂ (titration) on the same day

Ammonia measurements

Material and Reagents

All glassware has to be acid washed overnight!

- Glass test tubes (~25-mL) and racks
- Vortex mixer
- Micropipettes (10-100 μ L, 100-100 μ L)
- Macropipette (10-mL)
- 2 plastic cuvettes (1 cm)
- Spectrophotometer (640 nm)

All reagents are prepared according to standard method!

- Phenol solution (*max. age: 1 week*)
- Sodium nitroprusside solution (*max age: 1 month*)
- Oxidizing solution (*prepare fresh daily*)
- Standards: 20 μ g/L, 40 μ g/L, 100 μ g/L, 200 μ g/L, 400 μ g/L (*prepare fresh daily*)

Steps

- Let frozen samples thaw completely
- Dilute samples: suggested rate 1:250 (40 μ L sample in 10 mL milli-Q)
- Sample size: 10 mL
- Add 0.4 mL of Phenol solution, mix for 3-5 secs
- Add 0.4 mL of Sodium nitroprusside, mix for 3-5 secs
- Add 1 mL of Oxidizing solution, mix for 3-5 secs
- Cover samples and let color develop at room temperature in subdued light for at least 1 hr
- Measure absorbance at 640 nm against blank (milli-Q)

Remember to run replicates!

Titration (alkalinity, ΣCO_2)

Material and Reagents

Glassware should not be acid washed!

- Beakers (50-mL)
- PC-Titrator

- Titrant: 0.1 N HCl (*standardized according to standard method*)

Steps

- Calibrate pH-electrode (2 points)

- Setup “method file” or load stored file
[pat-alk.dfn
stability control: SLOPE, 15 secs, 0.010
end pH: adjust according to samples (≤ 3.5)
injection volume: set maximum ΔpH]

- Purge buret to remove air from tubing
- Rinse pH-electrode, temperature probe, stirrer with milli-Q

- Sample volume: 15 – 20 mL
- Start stirrer (10%)
- Start automatic titration
Do not forget to change default file name and sample volume!
- Wait until end pH has been exceeded or stop titration manually when enough data points are available

- Use Gran’s analysis to calculate volume to endpoint
perform manual analysis if $R^2 < 0.998$

Protocol: Algae culture

Material and Reagents

All glassware and pipette tips have to be autoclaved!

Use sterile techniques to avoid contamination of algae culture!

- Inoculation loop
- Erlenmeyer flasks (500-mL)
- Glass bottles (~12-L)
- Magnetic stir plates
- Tubing for aeration of algae cultures
- Incubator (25°C, 24-hr illumination)
- Nalgene centrifuge bottles (250-mL)
- Centrifuge

- Algal growth medium 4 x P
according to standard method, four times phosphorus
- *Selenastrum capricornutum* culture (on agar plate)
- NaCl solution (same conductivity as algae culture)

Start and maintain algae culture

- Inoculate 3 x 150 mL growth medium with algae
- Incubate for ~2 weeks or until starter cultures are noticeably green
- Use one starter culture per 12 L of growth medium
- Incubate algae culture for ~4 weeks or until enough algal biomass is available (green color)
- Stir and aerate constantly
Air has to be moistened by bubbling through distilled water!

Harvest algae

- Centrifuge algae culture:
 - 4 x 250 mL per run
 - 5000 – 6000 rpm
 - ~10 mins
- Discard supernatant
Repeat until entire algae culture has been reduced
- Resuspend algae in NaCl solution
- Centrifuge
Repeat resuspension step five times to remove dissolved nutrients
Freeze algae until needed

Appendix 4: Additional experimental results

This appendix is used to archive more detailed experimental results that were not included in the manuscript. Additional graphs are provided to better understand the experimental results, and experimental concerns and limitations are discussed.

Experimental concerns

Although this study examines variability of nutrient release rates among sediment types and the effects of substrate additions, it is not intended to yield in-situ decomposition rates. Sediment incubation experiments are a common method for studying the effects of environmental controls (e.g., organic matter quality or electron acceptor availability) on decomposition processes and nutrient dynamics (HOLMER, 1996; HULTHE et al., 1998; KRISTENSEN and HANSEN, 1995; KRISTENSEN and HOLMER, 2001; MATISOFF et al., 1981). Additional natural variability is eliminated by homogenizing the sediment samples prior to the incubation and by constant mixing during the course of the experiment. Aller and Mackin (1989) and Sun (1991) have shown that alterations of physical, chemical, and biological sediment properties caused by sample manipulation have only a short-term effect relative to the incubation period.

Changes in ammonium concentrations as a measure of N release rely on anaerobic conditions throughout the course of the incubation. If oxygen was available, nitrification and thus loss of ammonium could occur. Sediment homogenization and substrate amendments might introduce low levels of oxygen into the samples. Given typical rates of oxic decomposition, a pre-incubation period of approximately one day was estimated to be long enough to deplete all available oxygen.

The decomposition of organic matter requires electron acceptors. In marine sediments oxic respiration and sulfate reduction are the dominant pathways (HOWARTH and GIBLIN, 1983; HOWARTH and TEAL, 1979; HOWES et al., 1984). Lake water and sediments exhibit significantly lower sulfate concentrations leading to contributions of methanogenesis to organic matter breakdown of more than 70% (KELLY and RUDD, 1984; LOVLEY and KLUG, 1986). Since ΣCO_2 measurements were used to calculate C release rates, all sediment samples were amended with excess nitrate to inhibit methanogens (KRISTENSEN and HOLMER, 2001; LOVLEY and KLUG, 1986; LOVLEY and PHILLIPS, 1987).

DIC and DIN concentrations

The pH of all samples remained relatively constant over the entire incubation period with a maximum increase of 0.36 pH units for the algae-amended Dollar Bay sediment and a maximum decrease of 0.42 pH units for the Chassell Bay samples. The pH values were similar among different sediment types with a range of ~pH 6.1 to pH 6.5.

Unexpected rapid iron oxidation upon exposure to air interfered with alkalinity measurements for Dollar Bay, Chassell Bay, and Sturgeon Sloughs samples on the first day of sampling. Oxidation products (iron hydroxides) were observed as a reddish precipitate in all samples except Lily Pond. Magnetite formation was also observed on magnetic stir bars upon nitrate amendments indicating high iron concentrations in the sediments. The oxidation reaction liberates three H^+ ions for each Fe molecule and significantly lowers the pH of the samples and thus makes the alkalinity titration impossible. Starting on the second day of sampling, EDTA was added prior to the

centrifugation to complex reduced iron species. Stable pH values were obtained and proved the effectiveness of this addition.

Alkalinity and thus concentrations of total dissolved inorganic carbon (DIC) increased with time for all sediment types and all treatments. Initial DIC concentrations presented below are results of extrapolations from the second through fourth data point due to unexpected interference from iron oxidation on the first day of sampling. The estimations suggest significant variability with sediment type and amendment. The organic-matter-poor Sturgeon Sloughs sediment showed an initial concentration of $<10 \mu\text{mol C / g dry wt}$. Initial DIC in Dollar Bay sediment exceeded $40 \mu\text{mol C / g dry wt}$, and both Chassell Bay and Lily Pond showed intermediate values of $15\text{-}20 \mu\text{mol C / g dry wt}$. Glycine addition did not significantly alter the initial DIC concentration; the algae-amended Dollar Bay sediment exhibited a slightly increased value of $>50 \mu\text{mol C / g dry wt}$. The highest DIC concentration at the end of the incubation period was also measured in the algae-amended sample ($111 \mu\text{mol C / g dry wt}$; Figure 3-16 – Figure 3-29).

Both dissolved and adsorbed NH_3 increased during the incubation in all samples due to nitrogen mineralization. A similar linear relationship was found between the two fractions for all sediment types (Figure 3-30) suggesting that adsorption sites were not saturated at the existing NH_3 concentrations. Adsorbed NH_3 accounted for $\sim 30\text{-}50\%$ of total NH_3 ; no significant differences between sediment types were observed. Initial total NH_3 concentrations depend on sediment type and amendments. The lowest value was measured in the Sturgeon Sloughs sample ($0.79 \mu\text{mol N / g dry wt}$). Initial NH_3 in the Chassell Bay sediment was intermediate with $4.5 \mu\text{mol N / g dry wt}$, and Lily Pond and

Dollar Bay showed the highest concentrations with 7.0 $\mu\text{mol N / g dry wt}$ and 8.2 $\mu\text{mol N / g dry wt}$, respectively. Adding algae increased the initial concentration only slightly to 10.6 $\mu\text{mol N / g dry wt}$, whereas the small Glycine addition more than tripled the initial value (27.8 $\mu\text{mol N / g dry wt}$), and the large Glycine addition caused a more than five-fold increase (50.6 $\mu\text{mol N / g dry wt}$; Figure 3-16 – Figure 3-29). This strong increase is probably caused by direct ammonia formation from glycine hydrolysis; the amount of glycine lost via this pathway, however, was estimated to be <3.5% of the total glycine addition.

Substrate quality and C and N release rates

The effects of substrate quality and composition on sediment nutrient release were studied by comparing patterns of C and N release rates and their relation to sediment C and N contents. Regression analysis was used to calculate both carbon and nitrogen release rates. The release rate of inorganic nutrients corresponds to the concentration increase per time or the slope of the regression line. Variation of carbon release rates among the four sediment types is relatively small (Figure 3-31) and does not correlate with organic matter content. Nitrogen release, however, varies considerably among different sediment types (Figure 3-33) and is linearly correlated to sediment N contents (Figure 2-11). Since bulk C:N ratios are relatively similar for all four sediment types, the correlation between N release and N content is equivalent to a correlation between N release and organic matter content. An analogous simple relationship is not found for carbon release.

Amendments of sediment with labile material are a valuable tool to assess organic matter quality in sediments (see article for details). Fresh algal detritus generally

degrades much faster than sediment organic matter (WESTRICH and BERNER, 1984) and references cited therein). Small, soluble molecules such as amino acids have the highest decomposition rates reported (see HENRICHS, 1992) for review) and are therefore also suitable to simulate decomposition of labile material. The C:N ratio of green algae used in this study (~ 15 mol C / mol N) is higher than typical values for fresh phytoplankton indicating nitrogen deficiency in the growth medium or partial cell lysis prior to the addition. Leaching of nitrogen rich compounds while centrifuging and washing the algae culture might also have contributed to the higher C:N ratio.

All three amendments resulted in increased C release rates in comparison with the control (Figure 3-32). This general trend supports the assumption that decomposition rates are limited by the availability of labile material. Additions of labile substrate to sediments intensify microbial activity and thus induce higher mineralization rates. Analogously, nitrogen release was tripled in glycine-amended sediments and slightly enhanced due to the algal addition (Figure 3-34). Typical decomposition rates of labile (24 yr^{-1}) and stable (1.4 yr^{-1}) material (WESTRICH and BERNER, 1984) suggest that breakdown of labile substrate dominates carbon and nitrogen release during short-term incubations (< 50 days). For labile substrate additions linear relationships between changes in sediment C content and C release and N content and N release, respectively, are therefore expected. This correlation was only found for the algae amendment and the small glycine amendment.

Measured carbon and nitrogen release from large glycine amendment samples were markedly too low (Figure 3-35, Figure 3-36). This inconsistency in the glycine-amended samples cannot be fully explained from the data available. The reduced rates of C and N

release in the large glycine-amended samples might result from inhibition of microbial activity by high concentrations of labile substrate. Kristensen (1995) observed inhibition of anaerobic carbon mineralization in marine sediments amended with high concentrations of yeast. Kristensen's experiments, however, indicated that C and N mineralization were uncoupled at these high concentrations and that production of inorganic N was stimulated. Our data does not support this observation; both N and C release rates are lower than expected. Clearly, more experimental work is needed to fully understand the effects of high concentrations of labile, low-C:N material on C and N release.

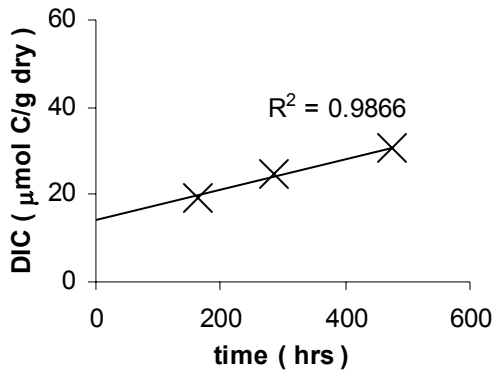


Figure 3-16 – Chassell Bay: DIC release

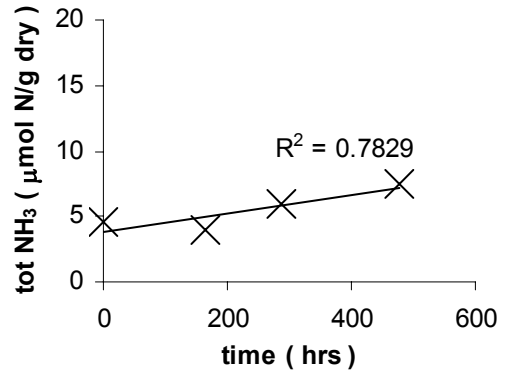


Figure 3-17 – Chassell Bay: DIN release

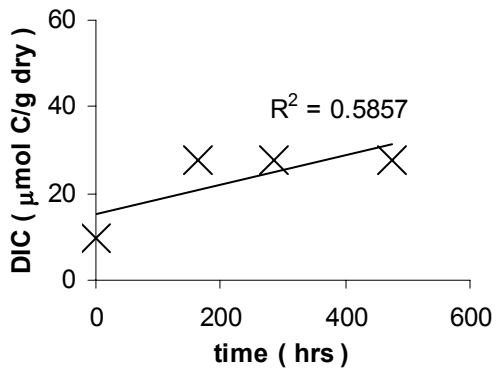


Figure 3-18 – Lily Pond: DIC release

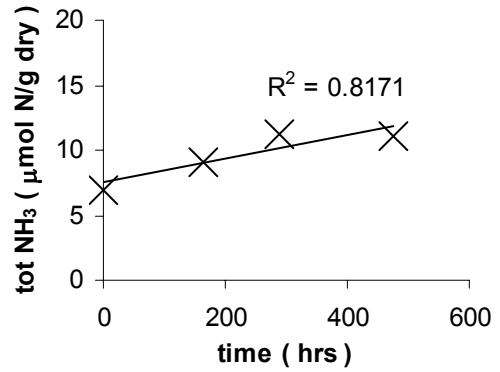


Figure 3-19 – Lily Pond: DIN release

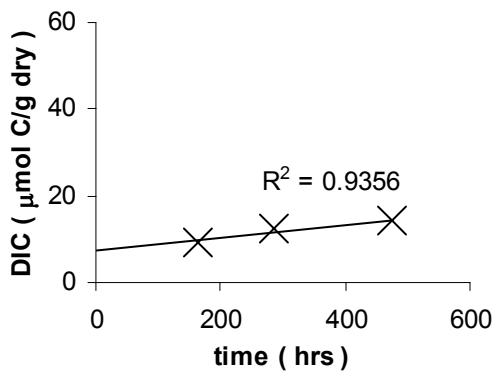


Figure 3-20 – Sturgeon Sloughs: DIC release

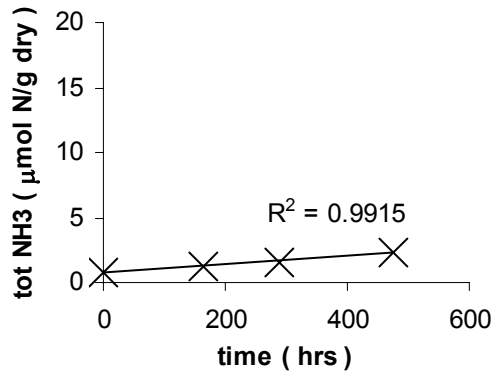


Figure 3-21 – Sturgeon Sloughs: DIN release

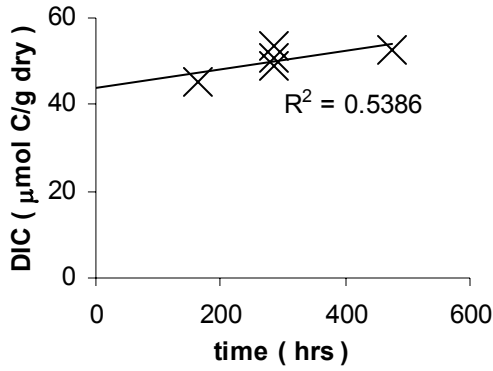


Figure 3-22 – Dollar Bay (DBC): DIC release

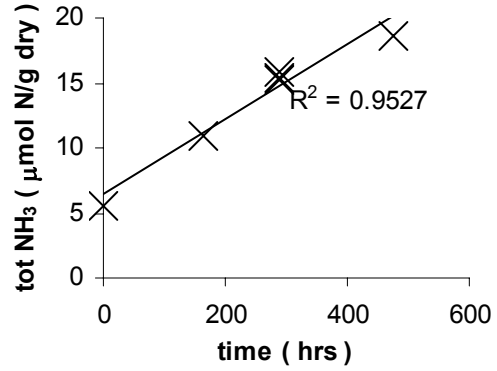


Figure 3-23 – Dollar Bay (DBC): DIN release

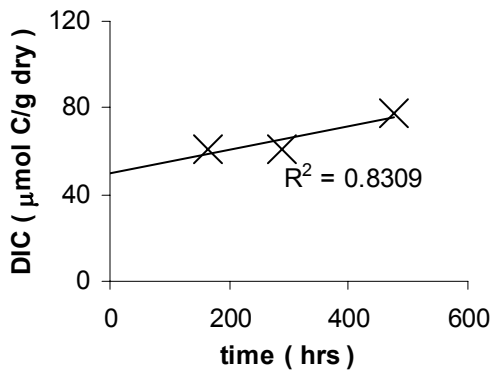


Figure 3-24 – Dollar Bay (DBLG): DIC release

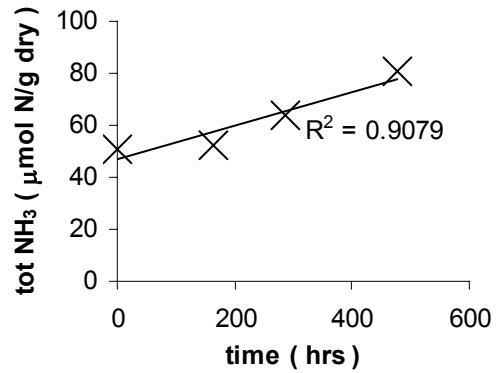


Figure 3-25 – Dollar Bay (DBLG): DIN release

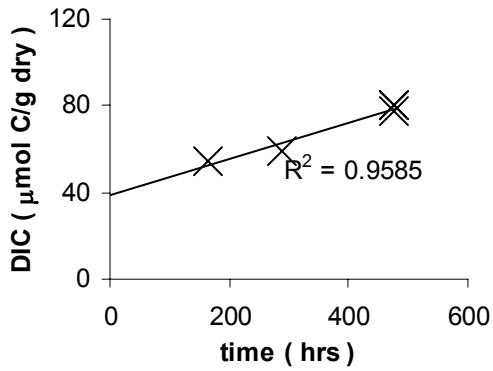


Figure 3-26 – Dollar Bay (DBSG): DIC release

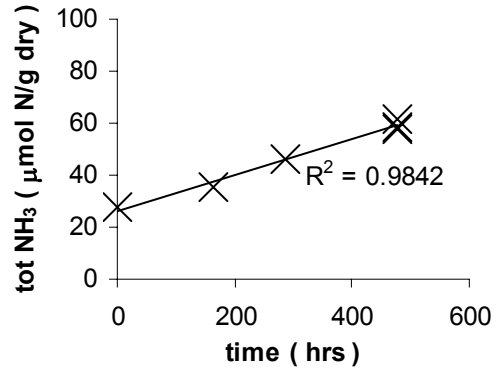


Figure 3-27 – Dollar Bay (DBSG): DIN release

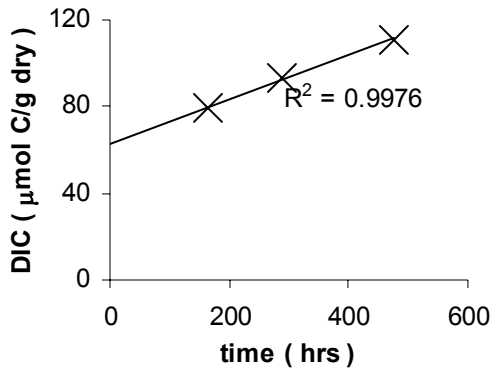


Figure 3-28 – Dollar Bay (DBA): DIC release

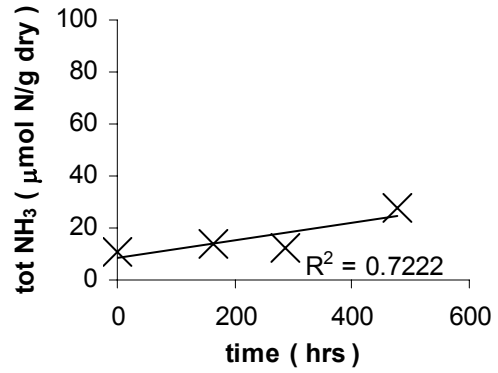


Figure 3-29 – Dollar Bay (DBA): N release

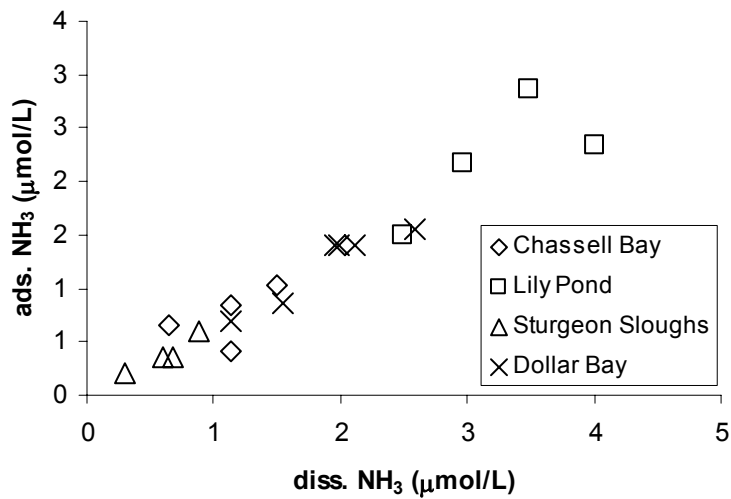


Figure 3-30 – Relationship between dissolved and adsorbed ammonium

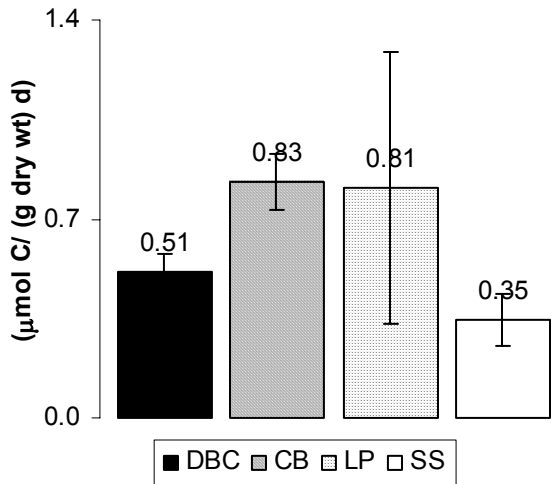


Figure 3-31 – Unamended sediments: C release rates (error bars = ± 1 standard error)

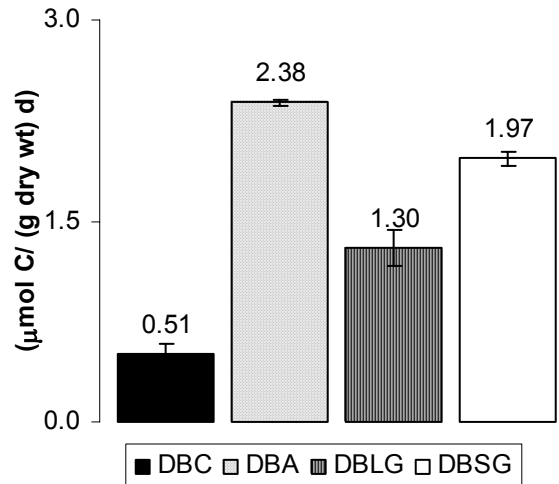


Figure 3-32 – Amended sediments: C release rates (error bars = ± 1 standard error)

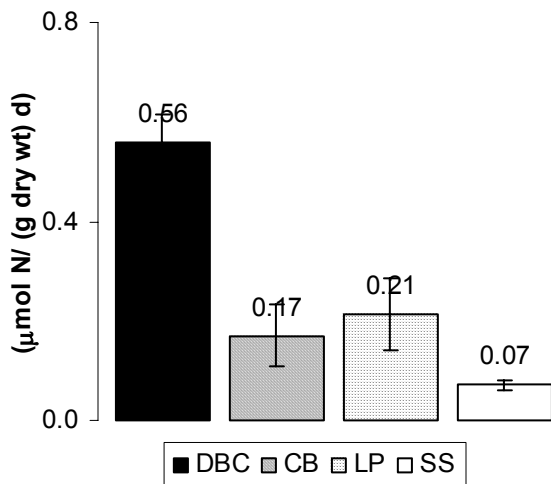


Figure 3-33 – Unamended sediments: N release rates (error bars = ± 1 standard error)

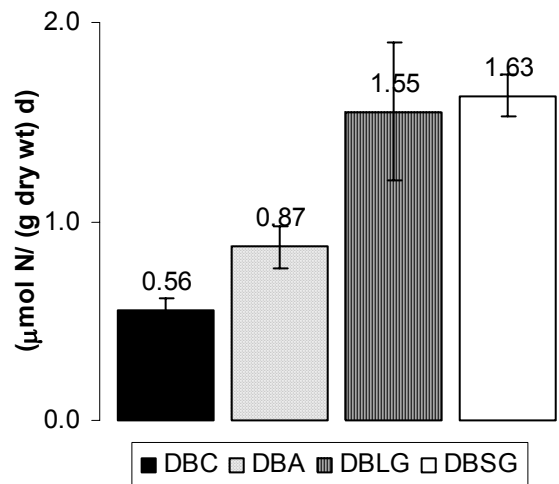


Figure 3-34 – Amended sediments: N release rates (error bars = ± 1 standard error)

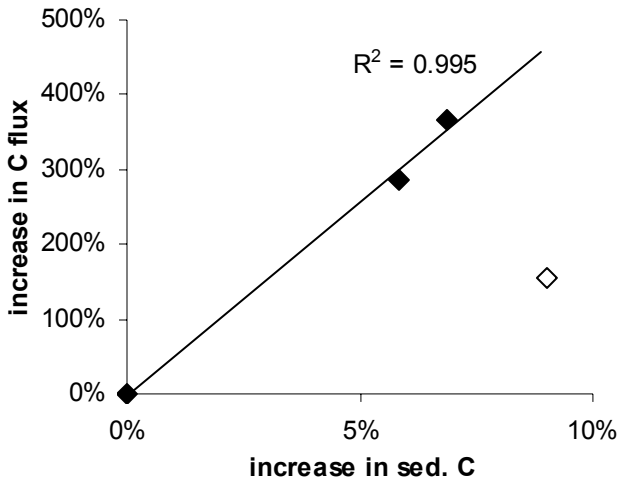


Figure 3-35 – Amended sediments: Increase in DIC flux vs. increase in sediment C content (DBLG omitted; open diamond)

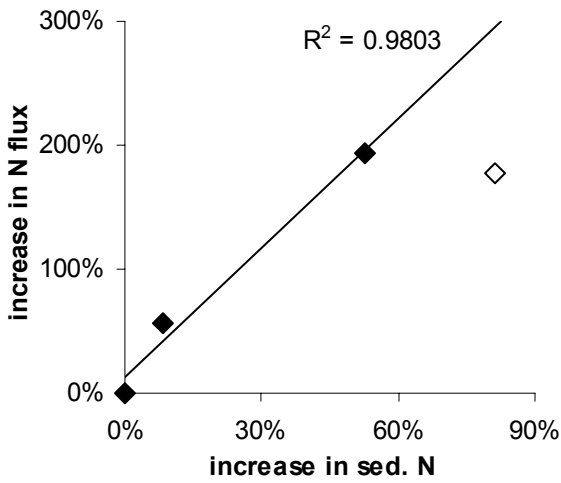


Figure 3-36 – Amended sediments: Increase in N flux vs. increase in sediment N content (DBLG omitted; open diamond)

Appendix 5: Visual Basic Code

Two-Box BIOSED model

Sub biomass ()

```
'-----  
  
'read in parameters  
  
    'modeling parameters  
  
        'calculation time step  
        dt = Cells(24, 7)  
  
        'simulation time period  
        T = Cells(25, 7)  
  
    'sediment properties  
        'solids concentration  
        m = Cells(5, 3)  
  
        'C:N of labile substrate  
        CNl = Cells(15, 3)  
  
        'C:N of stable substrate  
        CNs = Cells(16, 3)  
  
        'C:N of refractory substrate  
        CNr = Cells(17, 3)  
  
        'C:N of microbial biomass  
        CNb = Cells(18, 3)  
  
    'Box - In/Out - Transfer  
        'surface layer (Box1) thickness  
        H1 = Cells(9, 11)  
  
        'bottom layer (Box2) thickness  
        H2 = Cells(10, 11)  
  
        'burial velocity  
        w = Cells(11, 11)  
  
        'sedimentation flux (organic carbon)  
        Jc = Cells(13, 11)
```

```

    'fraction of labile material in input
      fl = Cells(14, 11)

    'fraction of stable material in input
      fs = Cells(15, 11)

    'fraction of refractory material in input
      fr = Cells(16, 11)

    'mass transfer coefficients
      'Box1 - water
        'DIC
          TC01 = Cells(19, 11)
        'DIN
          TC12 = Cells(20, 11)

      'Box2 - Box1
        'DIC
          TN01 = Cells(21, 11)
        'DIN
          TN12 = Cells(22, 11)

    'Decomposition
      'biomass normalization constant
        CbG = Cells(8, 7)

      'first-order rate constant (labile substrate)
        k1 = Cells(9, 7)

      'first-order rate constant (stable substrate)
        ks = Cells(10, 7)

      'C uptake efficiency
        eff = Cells(13, 7)

      'biomass recycling rate constant
        r = Cells(14, 7)
  -----

  'read in initial conditions

    'water
    CO20ini = Cells(24, 3)
    NH30ini = Cells(25, 3)

    'Box1
    Cl1ini = Cells(31, 3)
    Cs1ini = Cells(32, 3)
    Cr1ini = Cells(33, 3)
    Cb1ini = Cells(34, 3)
    CO21ini = Cells(35, 3)
    NH31ini = Cells(36, 3)

```

```
'Box2
Cl2ini = Cells(31, 6)
Cs2ini = Cells(32, 6)
Cr2ini = Cells(33, 6)
Cb2ini = Cells(34, 6)
CO22ini = Cells(35, 6)
NH32ini = Cells(36, 6)
```

'initialize variables

```
'water
  'inorganic carbon
    CO20 = CO20ini

  'inorganic nitrogen
    NH30 = NH30ini

'Box1
  'labile carbon
    C11 = C11ini

  'stable carbon
    Cs1 = Cs1ini

  'refractory carbon
    Cr1 = Cr1ini

  'biomass carbon
    Cb1 = Cb1ini

  'inorganic carbon
    CO21 = CO21ini

  'labile nitrogen
    N11 = C11 / CN1

  'stable nitrogen
    Ns1 = Cs1 / CNs

  'refractory nitrogen
    Nr1 = Cr1 / CNr

  'biomass nitrogen
    Nb1 = Cb1 / CNb

  'inorganic nitrogen
    NH31 = NH31ini
```

```

'Box2
    'analogous
        C12 = C12ini
        Cs2 = Cs2ini
        Cr2 = Cr2ini
        Cb2 = Cb2ini
        CO22 = CO22ini
        N12 = C12 / CN1
        Ns2 = Cs2 / CNS
        Nr2 = Cr2 / CNr
        Nb2 = Cb2 / CNb
        NH32 = NH32ini
'-----

'Model time stepping (step = 1 day)

For i = 0 To T

    'calculate fluxes (Box1 -> water)
        Cflux = TC01 * (CO21 - CO20)
        Nflux = TN01 * (NH31 - NH30)

    'calculate fluxes (Box2 -> Box1)
        Cflux2 = TC12 * (CO22 - CO21)
        Nflux2 = TN12 * (NH32 - NH31)

    'output
        'time
            Cells(i + 40, 1) = i

        'Box1
            Cells(i + 40, 2) = C11
            Cells(i + 40, 3) = Cs1
            Cells(i + 40, 4) = Cr1
            Cells(i + 40, 5) = Cb1
            Cells(i + 40, 6) = CO21

            Cells(i + 40, 7) = N11
            Cells(i + 40, 8) = Ns1
            Cells(i + 40, 9) = Nr1
            Cells(i + 40, 10) = Nb1
            Cells(i + 40, 11) = NH31

        'Box2
            Cells(i + 40, 14) = C12
            Cells(i + 40, 15) = Cs2
            Cells(i + 40, 16) = Cr2
            Cells(i + 40, 17) = Cb2
            Cells(i + 40, 18) = CO22

```

```

Cells(i + 40, 19) = N12
Cells(i + 40, 20) = Ns2
Cells(i + 40, 21) = Nr2
Cells(i + 40, 22) = Nb2
Cells(i + 40, 23) = NH32

'fluxes (Box1 -> water)
Cells(i + 40, 12) = Cflux
Cells(i + 40, 13) = Nflux

'fluxes (Box2 -> Box1)
Cells(i + 40, 24) = Cflux2
Cells(i + 40, 25) = Nflux2
'-----

'numerical integration (Euler method; step = dt)

For j = 0 To 1 / dt

'Box1
dC11 = (- (1 / eff) * (Cb1 / CbG) * k1 * C11 -
        (w * C11 / H1) + (f1 * Jc / H1) + (r * Cb1)) * dt

dCs1 = (- (1 / eff) * (Cb1 / CbG) * ks * Cs1 -
        (w * Cs1 / H1) + (fs * Jc / H1)) * dt

dCr1 = (- (w * Cr1 / H1) + (fr * Jc / H1)) * dt

dCb1 = ((Cb1 / CbG) * (k1 * C11 + ks * Cs1) -
        (w * Cb1 / H1) - (r * Cb1)) * dt

dCO21 = (((1 - eff) / eff) * (Cb1 / CbG) *
        (k1 * C11 + ks * Cs1) -
        TC01 * (CO21 - CO20) + TC12 * (CO22 - CO21)) * dt

dN11 = dC11 / CN1

dNs1 = dCs1 / CNs

dNr1 = dCr1 / CNr

dNb1 = dCb1 / CNb

dNH31 = ((Cb1 / CbG) *
        (k1 * C11 * ((1 / (eff * CN1)) - 1 / CNb) +
        ks * Cs1 * ((1 / (eff * CNs)) - 1 / CNb)) -
        TN01 * (NH31 - NH30) + TN12 * (NH32 - NH31)) * dt

```

```

'Box2
dCl2 =      (-(1 / eff) * (Cb2 / CbG) * kl * C12 -
             (w * C12 / H2) + (w * C11 / H2) + (r * Cb2)) * dt

dCs2 =      (-(1 / eff) * (Cb2 / CbG) * ks * Cs2 -
             (w * Cs2 / H2) + (w * Cs1 / H2)) * dt

dCr2 =      (-(w * Cr2 / H2) + (w * Cr1 / H2)) * dt

dCb2 =      ((Cb2 / CbG) * (kl * C12 + ks * Cs2) -
             (w * Cb2 / H2) + (w * Cb1 / H2) - (r * Cb2)) * dt

dCO22 =     ((Cb2 / CbG) *
             (kl * C12 * ((1 / (eff * CN1)) - 1 / CNb) +
             ks * Cs2 * ((1 / (eff * CNs)) - 1 / CNb)) -
             TC12 * (CO22 - CO21)) * dt

dN12 =      dCl2 / CN1

dNs2 =      dCs2 / CNs

dNr2 =      dCr2 / CNr

dNb2 =      dCb2 / CNb

dNH32 =     (((1 - eff) / eff) * (Cb2 / CbG) *
             (kl * C12 * ((1 / (eff * CN2)) - 1 / CNb) +
             ks * Cs1 * ((1 / (eff * CNs)) - 1 / CNb)) -
             TN12 * (NH32 - NH31)) * dt

```

```

'Box1
C11 = C11 + dC11
Cs1 = Cs1 + dCs1
Cr1 = Cr1 + dCr1
Cb1 = Cb1 + dCb1

CO21 = CO21 + dCO21

N11 = N11 + dN11
Ns1 = Ns1 + dNs1
Nr1 = Nr1 + dNr1
Nb1 = Nb1 + dNb1

NH31 = NH31 + dNH31

```

```
'Box2
  C12 = C12 + dC12
  Cs2 = Cs2 + dCs2
  Cr2 = Cr2 + dCr2
  Cb2 = Cb2 + dCb2

  CO22 = CO22 + dCO22

  N12 = N12 + dN12
  Ns2 = Ns2 + dNs2
  Nr2 = Nr2 + dNr2
  Nb2 = Nb2 + dNb2

  NH32 = NH32 + dNH32
```

'-----

```
Next j
Next i
```

End Sub

4. References

References

- Abrahamsen P. and Hansen S. (2000) Daisy: An open soil-crop-atmosphere system model. *Environmental Modelling and Software* **15**(3), 313-330.
- Aller R. C. and Mackin J. E. (1989) Open-incubation, diffusion methods for measuring solute reaction rates in sediments. *J. Mar. Res.* **47**(2), 411-440.
- Aller R. C. and Yingst J. Y. (1980) Relationships between microbial distributions and the anaerobic decomposition of organic matter in surface sediments of Long Island Sound, USA. *Marine Biology* **56**(1), 29-42.
- Berner R. A. (1980) *Early Diagenesis: A Theoretical Approach*. Princeton University Press, pp.241.
- Billen G. (1982) An idealized model of nitrogen recycling in marine sediments. *Amer. J. Sci.* **282**(4), 512-541.
- Bird R. B., Stewart W. E., and Lightfoot E. N. (1960) *Transport phenomena*. John Wiley & Sons, pp. 780.
- Blagodatsky S. A. and Richter O. (1998) Microbial growth in soil and nitrogen turnover: A theoretical model considering the activity state of microorganisms. *Soil Biol. Biochem.* **30**(13), 1743-1755.
- Bosatta E. and Ågren G. I. (1991) Dynamics of carbon and nitrogen in the organic matter of the soil: a generic theory. *American Naturalist* **138**(1), 227-245.
- Bosatta E. and Ågren G. I. (1999) Soil organic matter quality interpreted thermodynamically. *Soil Biol. Biochem.* **31**(13), 1889-1891.
- Boudreau B. P. (1996) *Diagenetic models and their implementation: modelling transport and reactions in aquatic sediments*. Springer, pp. 414.
- Boudreau B. P. and Marinelli R. L. (1994) A modelling study of discontinuous biological irrigation. *J. Mar. Res.* **52**, 947-968.
- Boudreau B. P. and Ruddick B. R. (1991) On a reactive continuum representation of organic matter diagenesis. *Amer. J. Sci.* **291**, 507-538.
- Burdige D. J. (1991) The kinetics of organic matter mineralization in anoxic marine sediments. *J. Mar. Res.* **49**(4), 727-761.
- Canfield D. E., Jørgensen B. B., Fossing H., Glud R., Gundersen J., Ramsing N. B., Thamdrup B., Hansen J. W., Nielsen L. P., and Hall P. O. (1993) Pathways of organic carbon oxidation in three continental margin sediments. *Marine Geology* **113**, 27-40.
- Capone D. G. and Kiene R. P. (1988) Comparison of microbial dynamics in marine and freshwater sediments: contrasts in anaerobic carbon catabolism. *Limnol. Oceanogr.* **33**(4), 725-749.
- Chapra S. C. (1997) *Surface water-quality modeling*. McGraw-Hill, pp. 844.

- Clesceri L. S., Eaton A. D., Greenberg A. E., and Franson M. A. H. (1998) *Standard methods for the examination of water and wastewater*. American Public Health Association.
- Davis M. B. and Ford M. S. (1982) Sediment focusing in Mirror Lake, New Hampshire. *Limnol. Oceanogr.* **27**(1), 137-150.
- Davison W. and Finlay B. J. (1986) Ferrous iron and phototrophy as alternative sinks for sulphide in the anoxic hypolimnia of two adjacent lakes. *J. Ecology* **74**, 663-673.
- Dean W. E. (1974) Determination of carbonate and organic matter in calcareous sediments and sedimentary rocks by loss on ignition: comparison with other methods. *Journal of Sedimentary Petrology* **44**, 242-248.
- Di Toro D. M. (2001) *Sediment flux modeling*. Wiley-Interscience, pp. 624.
- Engstrom D. R., Swain E. B., Henning T. A., Brigham M. E., and Brezonik P. L. (1994) Atmospheric Mercury Deposition to Lakes and Watersheds: A Quantitative Reconstruction from Multiple Sediment Cores. *Advances in Chemistry Series* **237**, 33-66.
- Erickson M. J. and Auer M. T. (1998) Chemical exchange at the sediment-water interface of Cannonsville Reservoir. *J. Lake and Reservoir Management* **14**, 266-277.
- Fenchel T., King G., and Blackburn T. H. (1998) *Bacterial biogeochemistry : the ecophysiology of mineral cycling*. Academic Press, pp. 307.
- Filippelli G. M. and Delaney M. L. (1996) Phosphorus geochemistry of equatorial Pacific sediments. *Geochim. Cosmochim. Acta* **60**(9), 1479-1495.
- Friedl G., Wehrli B., and Manceau A. (1997) Solid phases in the cycling of manganese in eutrophic lakes: new insights from EXAFS spectroscopy. *Geochim. Cosmochim. Acta* **61**(2), 275-290.
- Gächter R., Meyer J. S., and Mares A. (1988) Contribution of bacteria to release and fixation of phosphorus in lake sediments. *Limnol. Oceanogr.* **33**(6), 1542-1558.
- Gelda R. K., Auer M. T., and Effler S. W. (1995) Determination of sediment oxygen demand by direct measurement and by interference from reduced species accumulation. *Australian J. Marine and Freshwater Res.* **46**(1), 81-88.
- Goldman J. C. and Dennett M. R. (2000) Growth of marine bacteria in batch and continuous culture under carbon and nitrogen limitation. *Limnol. Oceanogr.* **45**(4), 789-800.
- Gorham E., Dean W. E., and Sanger J. E. (1983) The chemical composition of lakes in the north-central United States. *Limnol. Oceanogr.* **28**(2), 287-301.
- Gorham E., Lund J. W., Sanger J. E., and Dean W. E. (1974) Some relationships between algal standing crop, water chemistry, and sediment chemistry in the English Lakes. *Limnol. Oceanogr.* **19**, 601-617.

- Harvey H. R., Tuttle J. H., and Bell J. T. (1995) Kinetics of phytoplankton decay during simulated sedimentation: Changes in biochemical composition and microbial activity under oxic and anoxic conditions. *Geochim. Cosmochim. Acta* **59**(16), 3367-3377.
- Hedges J. I., Baldock J. A., Gelinas Y., Lee C., Peterson M., and Wakeham S. G. (2001) Evidence for nonn-selective preservation of organic matter in sinking marine particles. *Nature* **409**, 801-804.
- Henrichs S. M. (1992) Early diagenesis of organic matter in marine sediments: progress and perplexity. *Marine Chemistry* **39**(1-3), 119-149.
- Holmer M. (1996) Composition and fate of dissolved organic carbon derived from phytoplankton detritus in coastal marine sediments. *Mar. Ecol. Prog. Ser.* **141**(1-3), 217-228.
- Howarth R. W. and Giblin A. (1983) Sulfate Reduction in the Salt Marshes at Sapelo Island, Georgia. *Limnol. Oceanogr.* **28**, 70-82.
- Howarth R. W. and Teal J. M. (1979) Sulfate Reduction in an New England Salt Marsh. *Limnol. Oceanogr.* **24**, 999-1013.
- Howes B. L., Dacey J. W., and King G. M. (1984) Carbon flow through oxygen and sulfate reduction pathways in salt marsh sediments. *Limnol. Oceanogr.* **29**, 1037-1051.
- Hulthe G., Hulth S., and Hall P. O. J. (1998) Effect of oxygen on degradation rate of refractory and labile organic matter in continental margin sediments. *Geochim. Cosmochim. Acta* **62**(8), 1319-1328.
- Hunter K. S., Wang Y., and Van Cappellen P. (1998) Kinetic modeling of microbially-driven redox chemistry of subsurface environments: Coupling transport, microbial metabolism and geochemistry. *Journal of Hydrology* **209**(1-4), 53-80.
- Kelly C. A. and Rudd J. M. (1984) Epilimnetic sulfate reduction and its relationship to lake acidification. *Biogeochemistry* **1**, 63-77.
- Kelly-Gerreyn B. A., Hydes D. J., Trimmer M., and Nedwell D. B. (1999) Calibration of an early diagenesis model for high nitrate, low reactive sediments in a temperate latitude estuary (Great Ouse, Uk). *Mar. Ecol. Prog. Ser.* **177**, 37-50.
- Klump J. V. and Martens C. S. (1989) The seasonality of nutrient regeneration in an organic-rich coastal sediment: kinetic modeling of changing pore-water nutrient and sulfate distributions. *Limnol. Oceanogr.* **34**(3), 559-577.
- Kovarova-Kovar K. and Egli T. (1998) Growth Kinetics of Suspended Microbial Cells: From Single-Substrate-Controlled Growth to Mixed-Substrate Kinetics. *Microbiol. Mol. Biol. Rev.* **62**(3), 646-666.
- Kristensen E. and Hansen K. (1995) Decay of plant detritus in organic-poor marine sediment: Production rates and stoichiometry of dissolved C and N compounds. *J. Mar. Res.* **53**, 675-702.

- Kristensen E. and Holmer M. (2001) Decomposition of plant materials in marine sediment exposed to different electron acceptors (O₂, NO₃ and SO₄²⁻), with emphasis on substrate origin, degradation kinetics, and the role of bioturbation. *Geochim. Cosmochim. Acta* **65**(3), 419-433.
- Larsen D. P., Schults D. W., and Malereg K. W. (1981) Summer internal phosphorus supplies in Shagawa Lake, Minnesota. *Limnol. Oceanogr.* **26**, 740-753.
- Lehmann M. F., McKenzie J. A., Bernasconi S. M., and Barbieri A. (2002) Preservation of organic matter and alteration of its carbon and nitrogen isotope composition during simulated and in situ early sedimentary diagenesis. *Geochim. Cosmochim. Acta* **66**(20), 3573-3584.
- Lovley D. R. and Klug M. J. (1986) Model for the distribution of sulfate reduction and methanogenesis in freshwater sediments. *Geochim. Cosmochim. Acta* **50**(1), 11-18.
- Lovley D. R. and Phillips E. J. P. (1987) Competitive mechanisms for inhibition of sulfate reduction and methane production in the zone of ferric iron reduction in sediments. *Appl. Environ. Microbiol.* **53**, 2636-2641.
- Mackin J. E. and Aller R. C. (1984) Ammonium adsorption in marine sediments. *Limnol. Oceanogr.* **29**(2), 250-257.
- Matisoff G., Fisher J. B., and McCall P. (1981) Kinetics of nutrient and metal release from decomposing lake sediments. *Geochim. Cosmochim. Acta* **45**(12), 2333-2347.
- McGill W. B., Hunt H. W., Woodmansee R. G., and Reuss J. O. (1981) Phoenix, a model of the dynamics of carbon and nitrogen in grassland soils. In *Terrestrial Nitrogen Cycles. Processes, Ecosystem Strategies and Management Impacts*, Vol. 33 (ed. F. E. Clark, Rosswall, T.), pp. 49-115. Swedish Natural Science Research Council.
- Middelburg J. J. (1989) A simple rate model for organic matter decomposition in marine sediments. *Geochim. Cosmochim. Acta* **53**(7), 1577-1581.
- Monod J. (1942) *Recherches sur la croissance des cultures bacteriennes*. Hermann et Cie.
- NYC-DEP. (2000) <http://www.ci.nyc.ny.us/html/dep/html/wsmaps.html>. New York City Department of Environmental Protection.
- NYS. (2000) Reducing Harmful Phosphorus Pollution in the New York City Reservoirs through the Clean Water Act's "Total Maximum Daily Load" Requirements: A Case-Study of the New Croton Reservoir and Recommendation to EPA. Office of New York State Attorney General Eliot Spitzer.
- Park S. S. and Jaffé P. R. (1999) A Numerical Model to Estimate Sediment Oxygen Levels and Demand. *J. Environ. Qual.* **28**(4), 1219 (7 pages).
- Parnas H. (1975) Model for Decomposition of Organic Material by Microorganisms. *Soil Biol. Biochem.* **7**(2), 161-169.

- Parsons T. R., Maita Y., and Lalli C. M. (1984) *A manual of chemical and biological methods for seawater analysis*. Pergamon Press, pp. 173.
- Paul E. A. and Juma N. G. (1981) Mineralization and Immobilization of Soil Nitrogen by Microorganisms. In *Terrestrial Nitrogen Cycles. Processes, Ecosystem Strategies and Management Impacts*, Vol. 33 (ed. F. E. Clark, Rosswall, T.), pp. 179-195. Swedish Natural Science Research Council.
- Penn M. R., Auer M. T., Van Orman E. L., and Korienek J. J. (1995) Phosphorus diagenesis in lake sediments: investigations using fractionation techniques. *Mar. Freshwater Res.* **46**(1), 89-99.
- Rossi G. and Premazzi G. (1991) Delay in lake recovery caused by internal loading. *Water Research* **25**(5), 567-575.
- Rudd J. W., Kelly C. A., St.Louis V., Hesslein R. H., Furutani A., and Holoka M. H. (1986) Microbial consumption of nitric and sulfuric acids in acidified north temperate lakes. *Limnol. Oceanogr.* **31**, 1267-1280.
- Schmidt J. L., Deming J. W., Jumars P. A., and Keil R. G. (1998) Constancy of bacterial abundance in surficial marine sediments. *Limnol. Oceanogr.* **43**(5), 976-982.
- Soetaert K., Herman P. M. J., and Middelburg J. J. (1996) Dynamic response of deep-sea sediments to seasonal variations: A model. *Limnol. Oceanogr.* **41**(8), 1651 (18 pages).
- Solorzano L. (1969) Determination of ammonia in natural waters by phenolhypochlorite method. *Limnol. Oceanogr.* **14**, 799-801.
- Sun M.-Y., Aller R. C., and Lee C. (1991) Early diagenesis of chlorophyll-a in Long Island Sound sediments: a measure of carbon flux and particle reworking. *J. Mar. Res.* **49**(2), 379-401.
- Sweerts J. P. R. A., Bar-Gilissen M. J., Cornelese A. A., and Cappenberg T. E. (1991) Oxygen-consuming processes at the profundal and littoral sediment-water interface of a small meso-eutrophic lake (Lake Vechten, The Netherlands). *Limnol. Oceanogr.* **36**(6), 1124-1133.
- Tartari G. and Biasci G. (1997) Trophic status and lake sedimentation fluxes. *Water, Air, Soil Pollut.* **99**(1-4), 523-531.
- Thomann R. V. and Mueller J. A. (1987) *Principles of surface water quality modeling and control*. Harper & Row, pp. 644.
- Törnblom E. and Boström B. (1995) Benthic microbial response to a sedimentation event at low temperature in sediments of a eutrophic lake. *Mar. Freshwater Res.* **46**(1), 33-43.
- Tupas L. and Koike I. (1990) Amino acid and ammonium utilization by heterotrophic marine bacteria grown in enriched seawater. *Limnol. Oceanogr.* **35**(5), 1145-1155.

- Tupas L. and Koike I. (1991) Simultaneous uptake and regeneration of ammonium by mixed assemblages of heterotrophic marine bacteria. *Mar. Ecol. Prog. Ser.* **70**(3), 273.
- Urban N. R., Dinkel C., and Wehrli B. (1997) Solute transfer across the sediment surface of a eutrophic lake: I. Porewater profiles from dialysis samplers. *Aquatic Sciences* **59**(1), 1-25.
- Urban N. R., Gaechter R., and Bloesch J. (2002) The significance of C:N ratios in lacustrine particles. *Hydrobiologia* **submitted**.
- Urban N. R., Sampson C. J., Brezonik P. L., and Baker L. A. (2001) Sulfur cycling in the water column of Little Rock Lake, Wisconsin. *Biogeochemistry* **52**(1), 41-77.
- Van Cappellen P. and Yifeng W. (1996) Cycling of iron and manganese in surface sediments: a general theory for the coupled transport and reaction of carbon, oxygen, nitrogen, sulfur, iron, and manganese. *Amer. J. Sci.* **296**(3), 197-243.
- Van Veen J. A., McGill W. B., Hunt H. W., Frissel M. J., and Cole C. V. (1981) Simulation Models Of The Terrestrial Nitrogen Cycle. In *Terrestrial Nitrogen Cycles. Processes, Ecosystem Strategies and Management Impacts*, Vol. 33 (ed. F. E. Clark, Rosswall, T.), pp. 25-48. Swedish Natural Science Research Council.
- Wang Y. and Van Cappellen P. (1996) A multicomponent reactive transport model of early diagenesis: application to redox cycling in coastal marine sediments. *Geochim. Cosmochim. Acta* **60**(16), 2993-3014.
- Welch E. B., Spyridakis D. E., Shuster J. I., and Horner R. R. (1986) Declining lake sediment phosphorus release and oxygen deficit following wastewater diversion. *J. Water Pollut. Control Fed.* **58**, 92-96.
- Westrich J. T. and Berner R. A. (1984) The role of sedimentary organic matter in bacterial sulfate reduction: the G model tested. *Limnol. Oceanogr.* **29**(2), 236-249.